UNCLASSIFIED
SECURITY CLASSIFICATION OF THIS PAGE

REPORT DOCUMENTATION PAGE

1a. REPORT SECURITY CLASSIFICATION UNCLASSIFIED	1b. RESTRICTIVE MARKINGS
2a. SECURITY CLASSIFICATION AUTHORITY	3. DISTRIBUTION / AVAILABILITY OF REPORT Approved for public release; distribution unlimited.
2b. DECLASSIFICATION / DOWNGRADING SCHEDULE	
4. PERFORMING ORGANIZATION REPORT NUMBER(S) TR 7511	5. MONITORING ORGANIZATION REPORT NUMBER(S)
6a. NAME OF PERFORMING ORGANIZATION Naval Underwater Systems Center 6b. OFFICE SYMBOL (If applicable)	7a. NAME OF MONITORING ORGANIZATION
6c. ADDRESS (City, State, and ZIP Code). New London Laboratory New London, Connecticut 06320	7b. ADDRESS (City, State, and ZIP Code)
8a. NAME OF FUNDING / SPONSORING ORGANIZATION 8b. OFFICE SYMBOL (If applicable)	9. PROCUREMENT INSTRUMENT IDENTIFICATION NUMBER
8c. ADDRESS (City, State, and ZIP Code)	10. SOURCE OF FUNDING NUMBERS PROGRAM ELEMENT NO. / PROJECT NO. ZR0000101 / TASK NO. / WORK UNIT ACCESSION NO.

11. TITLE (Include Security Classification)
SPECTRAL ANALYSIS VIA LAG-RESHAPING OF THE CORRELATION ESTIMATE; PROGRAMS AND SIMULATION RESULTS

12. PERSONAL AUTHOR(S)
Albert H. Nuttall

13a. TYPE OF REPORT	13b. TIME COVERED FROM _____ TO _____	14. DATE OF REPORT (Year, Month, Day)	15. PAGE COUNT
		16 August 1985	

16. SUPPLEMENTARY NOTATION

17. COSATI CODES			18. SUBJECT TERMS (Continue on reverse if necessary and identify by block number)
FIELD	GROUP	SUB-GROUP	Effective Window, Lag Weighting, FFT Processing, Minimum Execution Time, Lag-Reshaping, Minimum Variance

19. ABSTRACT (Continue on reverse if necessary and identify by block number)

The possibility of achieving maximally stable, low-sidelobe spectral estimates, without the need for temporal overlapping or weighting, is investigated and confirmed via simulation. In particular, the (frequency domain) power spectral estimates of each of a sequence of abutting, rectangularly gated, time data segments are averaged and then Fourier transformed into the lag (or correlation) domain. This correlation estimate is then reshaped, by dividing out the undesirable triangular autocorrelation of the rectangular temporal weighting, and by multiplying by a desirable lag-weighting function with low sidelobes and adequate decay. Another Fourier transform yields the final spectral estimate of interest. Multiple spectral analyses with different resolution bandwidths are easily achieved by changing just the final lag weighting and doing one additional FFT for each case of interest.

20. DISTRIBUTION / AVAILABILITY OF ABSTRACT	21. ABSTRACT SECURITY CLASSIFICATION
☒ UNCLASSIFIED/UNLIMITED ☐ SAME AS RPT. ☐ DTIC USERS	UNCLASSIFIED
22a. NAME OF RESPONSIBLE INDIVIDUAL Albert H. Nuttall	22b. TELEPHONE (Include Area Code) 203-440-4618 / 22c. OFFICE SYMBOL Code 3314

DD FORM 1473, 84 MAR 83 APR edition may be used until exhausted. All other editions are obsolete.

SECURITY CLASSIFICATION OF THIS PAGE
UNCLASSIFIED

18. (Cont'd)

Normalized Quality Ratio	Spectral Analysis
Resolution vs. Stability	Stable Spectral Estimates
Segment Averaging	Temporal Weighting
Sidelobe Control	Tones in Noise
Simulation	Wrap-Around

19. (Cont'd)

The mean of the spectral estimate is equal to the convolution of the true spectrum of the data with an effective window. In the case of lag-reshaping, the effective window corresponds directly with the desirable lag weighting function above, with its low sidelobes. More generally, the effective window is equal to the convolution of the lag window with the magnitude-squared temporal window. Previous analytic results for the variance of the spectral estimate with rectangular temporal weighting indicate that, if the length of the temporal weighting is selected to be somewhat larger than the length of the lag weighting, the variance is at a near minimum. Furthermore, in this situation, the possibly deleterious sidelobes of the temporal weighting can be exactly compensated by proper choice of lag weighting, resulting in low sidelobes and good decay of the overall effective spectral window.

Programs for achieving lag-reshaping spectral analysis are presented for complex data as well as for real data. Timing results and recommendations for minimizing execution time, subject to a specified frequency resolution, are given. Simulation results that confirm all the effects predicted theoretically are presented. The possibility of detecting a weak tonal via lag-reshaping is demonstrated, both for a nearby frequency as well as a distant tonal.

NUSC Technical Report 7511
16 August 1985

Spectral Analysis via Lag-Reshaping of the Correlation Estimate; Programs and Simulation Results

Albert H. Nuttall
Surface Ship Sonar Department

Naval Underwater Systems Center
Newport, Rhode Island / New London, Connecticut

PREFACE

This research was conducted under NUSC Project No. A75205, Subproject No. ZR0000101, "Applications of Statistical Communication Theory to Acoustic Signal Processing," Principal Investigator Dr. Albert H. Nuttall (Code 33), Program Manager Gary Morton, Director of Navy Laboratories.

The author would like to acknowledge several helpful discussions with the Technical Reviewer of this report, Dr. G. C. Carter (Code 3314).

Reviewed and Approved: 16 August 1985

W. A. Von Winkle
Associate Technical Director for Technology

The author of this report is located at the
New London Laboratory, Naval Underwater Systems Center,
New London, Connecticut 06320.

TABLE OF CONTENTS

LIST OF ILLUSTRATIONS

LIST OF SYMBOLS

T	available record length in seconds
B_e	effective frequency resolution in hertz, (1) and (18)
t	time
$x(t)$	data record
f	frequency
$G(f)$	true (unknown) spectrum of $x(t)$
$W_o(f)$	spectral window
$H(f)$	filter voltage transfer function
P	estimate of power
Q	quality ratio, (2)
$Av(P)$	average value of random variable P
$Var(P)$	variance of random variable P
overbar	ensemble average
NQR	normalized quality ratio
Δ_t	sampling increment (= 1 second)
K	number of pieces of data
L_1	length of each data segment
n	time sample number
$x_n^{(k)}$	k-th data segment at time n, (5)
$X_m^{(k)}$	k-th FFT at frequency bin m, (6)
N_1	size of first-stage FFT
A_m	first-stage spectral estimate, (9)

LIST OF SYMBOLS (cont'd)

a_n	first-stage correlation estimate, (10)
w_n	lag weighting, figure 3
L_2	lag weighting length, figure 3 and (12)
b_n	second-stage correlation estimate, (12)
$w_n^{(d)}$	desirable lag weighting, (13)
B_m	second-stage spectral estimate, (15)
N_2	size of second-stage FFT
P_T	sample power of total data record, (20)
α_k	lag weighting coefficient, (21)
C1	continuous first derivative, (22)
$L_2(max)$	maximum lag weighting length of interest
f_m	frequency m/N_2
I_n	dimensionless constants, (39)
T_n	auxiliary constants, (41)

SPECTRAL ANALYSIS VIA LAG-RESHAPING OF THE CORRELATION ESTIMATE; PROGRAMS AND SIMULATION RESULTS

INTRODUCTION

The fundamental performance of the generalized spectral analysis technique employing quadratic frequency-smoothing of Fourier-transformed, overlapped, weighted data segments was thoroughly investigated analytically and reported in [1]. One attractive possibility pointed out there was that of doing lag-reshaping of the first-stage correlation estimate, and thereby realizing effective spectral windows with low sidelobes and good decay rates, without the need for overlap or any temporal weighting at all. However, no programs or simulation results for this particular technique were presented at that time. We rectify this situation here by presenting programs for achieving maximally stable low-sidelobe spectral estimates via the lag-reshaping procedure [1, pages 36-40] and then employ these routines to exhibit some simulation results for data with tones and noise.

Spectral analysis techniques have received a great deal of attention in the past [2 - 13], ranging from the original autocorrelation approach of Blackman-Tukey [3] to the more recent weighted, overlapped, segment-averaging FFT approach [8 - 13]. These two apparently disparate approaches are limiting special cases of a generalized framework [1] for spectral analysis; thus consideration of this general technique elucidates the fundamental behavior

and performance of a rather wide variety of spectral approaches and their tradeoffs. This generalized framework was originally presented in [14 - 16], where a brief summary of some of the main features was mentioned. The analytical results, detailed derivations, and quantitative results were given in [1].

There are two fundamental parameters that critically affect the performance of any spectral estimation technique. They are the available record length, T, of the stationary random process under investigation, and the effective frequency resolution, B_e, of the technique under consideration. We would like to be able to attain fine resolution (small B_e) with short data lengths and storage (small T); however, stable results (small fluctuations) are achievable only if the product TB_e is much larger than unity. The problems of interest are how to make optimum use of a given limited amount of data, in order to realize a specified desired resolution with maximum stability, and to determine what tradeoffs are available regarding windowing and weighting at different stages of the spectral analysis procedure. It is assumed that the reader is familiar with the tradeoffs presented in [10] for the weighted, overlapped, segment-averaging FFT procedure, and with the concepts and results of the generalized framework in [1].

In this report, we will confine attention solely to the case of abutting rectangular temporal weightings with no overlap; this procedure, with appropriate lag-reshaping, has been shown [1, pages 48-50 and 58] to have

excellent effective spectral windows (low sidelobes and rapid decay) and virtually ideal variance reduction capability, under proper choice of the lag weighting and the ratio of weighting lengths. Furthermore, it requires no temporal multiplications whatsoever on the given data, and it avoids the additional manipulations associated with overlapped data segments. Thus it is a strong candidate for consideration in spectral analysis.

Separate programs for spectral analysis of complex data as well as real data are presented here. Also, the programs are written in such a fashion that if multiple frequency-resolution bandwidths are desired, they can be easily accommodated without re-doing the bulk of the required data processing; in fact, one new lag weighting and one FFT will suffice for each different required resolution.

Although the present programs and study are limited to auto-spectral analysis, they can be easily generalized to incorporate cross-spectral analysis if desired, both for complex as well as real data. The present conclusions on execution time and stability should carry over directly to this more general case.

ULTIMATE STABILITY ATTAINABLE FROM A GIVEN RECORD LENGTH

Suppose a stationary (complex) data record x(t) of length T seconds is available and that we wish to estimate its power density spectrum G(f) at frequency f, with an effective frequency resolution of B_e Hz, where $W_o(f)$ is the narrowband window through which the power density spectrum is to be observed. These two frequency-domain quantities are related according to

$$B_e = \frac{\left[\int df\ W_o(f)\right]^2}{\int df\ W_o^2(f)} \quad . \tag{1}$$

This bandwidth measure, B_e, is called the statistical bandwidth of $W_o(f)$ in [6, page 265]. The relation of effective bandwidth B_e to the half-power bandwidth is considered in [1, appendix A]; it is shown that for good windows, the ratio of the two bandwidths is relatively independent of the exact window shape. Thus it is possible to translate results to other bandwidth measures without significantly affecting the essential quantitative aspects.

If we take the original data record and pass it through a narrowband linear (complex) filter with power transfer function equal to the window, $|H(f)|^2 = W_o(f)$, and which is centered at a frequency, f_o, of interest, we will have lost no relevant information about the process in the frequency band of interest, because we have filtered out information of no use. We can

now estimate the power in the narrowband filter output process and use it as a measure of the spectrum of the input process in the neighborhood of frequency f_o; see figure 1.

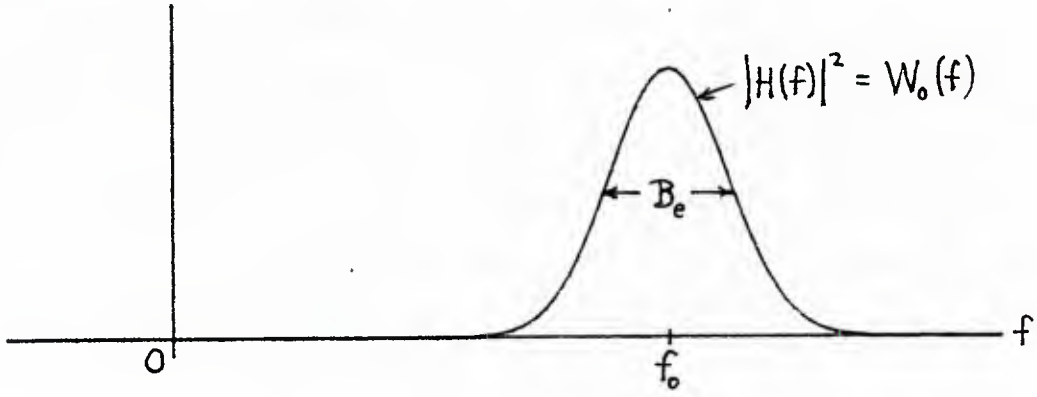

Figure 1. Power Transfer Function of Narrowband Linear Filter H(f)

A quality ratio can be defined for the power estimate P at the filter output as

$$Q = \frac{Var(P)}{Av^2(P)} = \frac{\overline{P^2} - \overline{P}^2}{\overline{P}^2} , \tag{2}$$

where the overbar denotes an ensemble average. Under the assumptions that the filter input spectrum G(f) does not vary rapidly with respect to bandwidth B_e, that the observation-time resolution-bandwidth product TB_e is large, and that the filter output is approximately Gaussian, it is shown in [1, pages 3-5] that

$$Q = \frac{1}{TB_e} . \tag{3}$$

This is the smallest value of quality ratio Q, for specified resolution B_e and available record length T; no other spectral analysis procedure can outperform this benchmark. Thus (3) serves as a very useful comparison standard for any technique and will be employed here in the stability investigation. Specifically, the normalized quality ratio (NQR) for a particular technique is defined as the quotient of the quality ratio of that technique, (2), relative to the minimum value in (3). Thus NQR is always greater than unity, with small values being desirable.

SPECTRAL ANALYSIS PROCEDURE

The available stationary data process x(t) is presumed to be sampled at unit time increment, for convenience; that is, $\Delta_t = 1$ second in [1, (24) et seq.]. There should be no problem in scaling these results to a general time sampling increment Δ_t. Thus the observation time T measures both the available data record length and the number of available data points.

This total of T data points is broken into K abutting non-overlapping data segments each of length L_1; thus

$$T = K L_1 , \tag{4}$$

where L_1 is the length of the (rectangular) temporal weighting. The data points in the k-th piece, $1 \leq k \leq K$, are labeled $\left\{x_n^{(k)}\right\}$ for $0 \leq n \leq L_1 - 1$, where n is a time index; thus in terms of original process x(t), we have (since $\Delta_t = 1$)

$$x_n^{(k)} = x\left(n+(k-1)L_1\right) \quad \text{for } 0 \leq n \leq L_1 - 1 , \quad 1 \leq k \leq K . \tag{5}$$

Notice there are no common data points in any of the different pieces.

FIRST-STAGE ESTIMATES

According to the procedure described in [1], we perform a forward N_1-point (first-stage) FFT of each piece of data (N_1 = power of 2):

$$X_m^{(k)} = \sum_{n=0}^{L_1-1} \exp(-i2\pi nm/N_1)\, x_n^{(k)} \quad \text{for } 0 \le m \le N_1 - 1, \quad 1 \le k \le K, \tag{6}$$

where m is a frequency bin index. Observe that no temporal weighting is employed on the available data. We presume that FFT size N_1 and segment length L_1 are chosen to satisfy constraint

$$N_1 \ge L_1 \, . \tag{7}$$

However, we will discover shortly that N_1 must be chosen even larger than constraint (7); thus some zero-filling is required in (6), namely, $N_1 - L_1$ zeros, prior to taking the FFT dictated by (6). The spacing of the frequency domain components $\left\{X_m^{(k)}\right\}$ in (6) is

$$\frac{1}{N_1 \Delta_t} = \frac{1}{N_1} \text{ Hz}, \tag{8}$$

and they cover a total band of $1/\Delta_t = 1$ Hz. Thus the m-th frequency component in (6) is at frequency m/N_1 Hz.

The frequency components in (6) are now subjected to a magnitude-square operation and segment-averaging over the available K pieces of data, yielding the first-stage spectral estimates

$$A_m = \sum_{k=1}^{K} \left|X_m^{(k)}\right|^2 \quad \text{for } 0 \le m \le N_1 - 1. \tag{9}$$

(Scale factors will be accounted for later, at the end of the spectral procedure description.) These power spectral estimates also occur at the frequency spacing indicated in (8), and cover a total band of 1 Hz.

We now inverse Fourier transform (9) back into the lag domain, obtaining first-stage correlation estimates defined as

$$a_n = \sum_{m=0}^{N_1-1} \exp(i2\pi nm/N_1)\, A_m \quad \text{for all } n. \tag{10}$$

This is an N_1-point transform; however, we let it define the sequence $\{a_n\}$ for all n, with period N_1. The spacing of correlation estimates $\{a_n\}$ in the lag domain is Δ_t = 1 second. A typical representative plot of $\{a_n\}$ in figure 2 reveals an important property of correlation estimates obtained via the forward-and-inverse discrete Fourier transform procedure of (6)-(10):

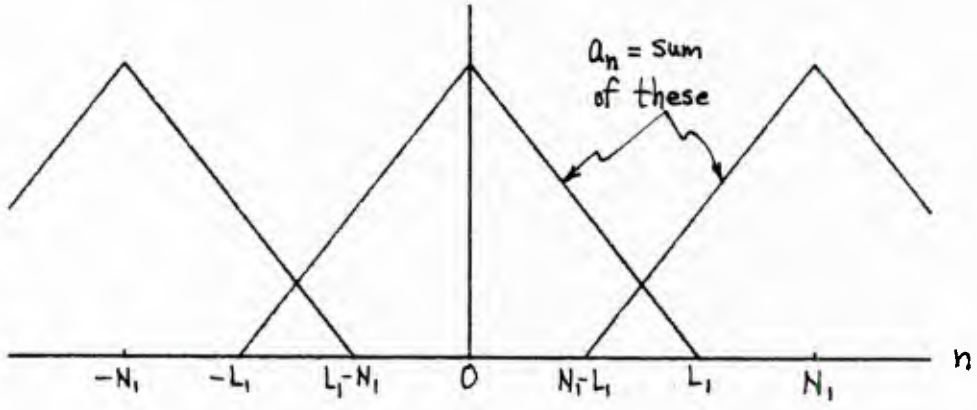

Figure 2. Wrap-Around in the Lag Domain

Namely, $\{a_n\}$ equals the periodic correlation of a data sequence of length L_1; unless $N_1 \geq 2L_1$, $\{a_n\}$ will suffer wrap-around, since each a_n is the sum of all the displaced periodic versions of the desired aperiodic correlation (the triangle centered at n = 0). However, we can still tolerate some wrap-around, if the lag weighting length L_2 is chosen small enough, as indicated in figure 3:

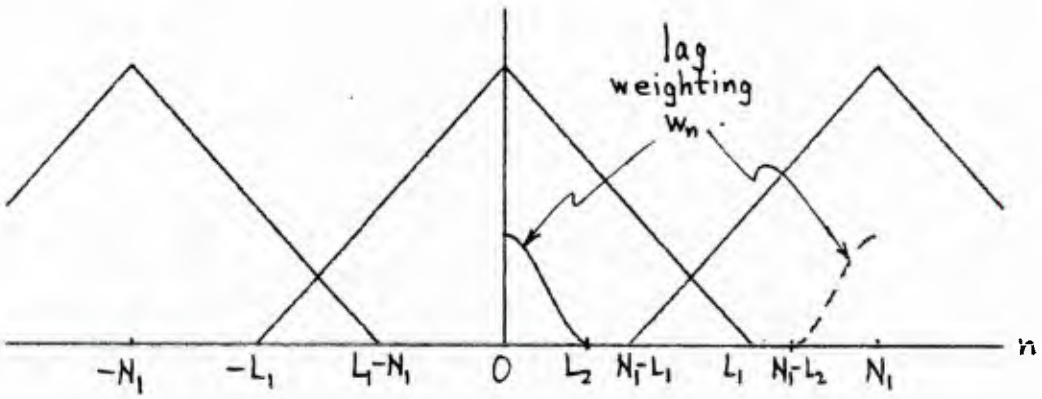

Figure 3. Allowed Lag Weighting to Suppress Wrap-Around

Thus, if

$$L_2 \leq N_1 - L_1 , \quad \text{i.e.,} \quad N_1 \geq L_1 + L_2 , \tag{11}$$

then the lag weighting w_n goes to zero before any undesired overlap occurs from the aliasing lobes centered at $n = \pm N_1$. This ability to get unaliased correlation estimates via an FFT approach was also pointed out and utilized in

[1, page 12, (41) et seq.] and [17, (15)]. The constraint in (11) will be developed even further when we discuss execution time and stability of the final spectral estimate.

The constraint in (11) is not an upper bound on L_1 and L_2, as much as it is a lower bound on N_1. That is, if we want to estimate the correlation of the input data via this forward-and-inverse FFT approach (for minimum execution time reasons), we must choose the first-stage FFT size, $N_1 \geq L_1 + L_2$, in order to circumvent the inherent wrap-around associated with the procedure. By contrast, recognize that if we calculated the correlation of the available input data by the brute force delay-multiply-add procedure (Blackman-Tukey), no such limitation would arise; we would simply compute correlation estimates to the maximum lag L_2 of interest. Since finer frequency resolution of the final (second-stage) spectral estimates is achieved by making lag L_2 larger, the size N_1 of the first-stage FFT will have to be increased accordingly; in fact, it must accommodate the largest L_2 of interest in the second-stage estimation procedure.

SECOND-STAGE ESTIMATES

The second-stage correlation estimates are obtained by lag weighting the first-stage estimates in (10):

$$b_n = w_n a_n \quad \text{for } 0 \leq n \leq L_2 < L_1 \; . \tag{12}$$

Here lag weighting coefficients w_n are selected according to

$$w_n = \frac{w_n^{(d)}}{1 - \frac{n}{L_1}} \quad \text{for } 0 \leq n \leq L_2 < L_1 \ , \tag{13}$$

where the numerator is a desirable lag weighting with low sidelobes and adequate decay, while the denominator is the autocorrelation of the rectangular temporal weighting employed in transform (6); see [1, (36)-(40)].

Actually, since transform (10) will be accomplished via an FFT, the values of $\{a_n\}$ for $0 \leq n \leq N_1 - 1$ will be stored and available, while values for $n < 0$ will not be. Accordingly, the weighting in (12) and (13) must be augmented to account for a symmetric weighting about $n = 0$. This is accomplished by also weighting the upper end of the $\{a_n\}$ sequence near $n = N_1$, as indicated by the dashed curve in figure 3. The same constraint (11) suffices to guarantee no effect due to aliasing from the tail of the correlation lobe which is centered at $n = 0$.

Although we only need to compute $\{a_n\}$ up through L_2, since lag weighting w_n is zero beyond there, the FFT will yield N_1 values of a_n via (10). The excess values not required in figure 3 are simply discarded. Also, advantage can be taken of the conjugate symmetry of a_n about $n = 0$, $\pm N_1$, etc.; i.e., $a_{-n} = a_n^*$ since a_n is a correlation estimate.

The application of lag weighting (13) in (12) can be accomplished in two steps:

$$b_n = w_n^{(d)} \frac{a_n}{1 - \frac{n}{L_1}} \quad \text{for } 0 \le n \le L_2 < L_1 \ . \tag{14}$$

The reason for this separation of effort is that the division of a_n by $1 - n/L_1$ can be done once, prior to knowledge or selection of L_2 and $w_n^{(d)}$, stored, and then re-used for several different desirable lag weightings $w_n^{(d)}$, which can have different lengths L_2 and/or sidelobe character and decay, for whatever frequency resolution is of interest. Good candidate lag weightings in this respect are the optimum ones presented in [18]. The restriction that $L_2 < L_1$ in (14) is necessary to avoid a division by zero at $n = L_2$.

Finally, the second-stage spectral estimates are obtained by transforming (12) into the frequency domain (N_2 = power of 2):

$$B_m = \sum_{n=0}^{L_2} \exp(-i2\pi nm/N_2)\ b_n \quad \text{for } 0 \le m \le N_2 - 1 \ . \tag{15}$$

The size of this final FFT dictates the frequency spacing of these spectral estimates, namely,

$$\frac{1}{N_2 \Delta_t} = \frac{1}{N_2} \ \text{Hz} \ . \tag{16}$$

Thus the m-th frequency component in (15) is at frequency $f_m = m/N_2$ Hz. In order to be able to observe all the detail of the second-stage estimate, we should choose

$$N_2 >> L_2 \ . \tag{17}$$

However, N_2 has no effect on the stability or resolution capability of spectral estimates $\{B_m\}$; rather, the stability depends on L_2/L_1 and L_2/T, while the frequency resolution is [1, (101) and table 1]

$$B_e = \frac{1}{2\, c\{w_d\}\, L_2} \approx \frac{2}{L_2} \text{ Hz} . \tag{18}$$

(The exact factor depends on the particular weighting employed.) The maximum value of the lag weighting length, $L_2(\max)$, should therefore be chosen to achieve the finest frequency resolution required; smaller values of L_2 will then result in coarser, but more stable estimates.

It can be seen from the above considerations that FFT sizes N_1 and N_2 in (6) and (15), respectively, play subordinate roles insofar as the fundamental capabilities of this spectral analysis technique are concerned; they are parameters of the "tool" (i.e., the FFT) being used to obtain the spectral estimates, and must satisfy constraints (11) and (17), but are otherwise arbitrary. The fundamental parameters are T, L_1, and L_2.

SCALING

If we sum up the power spectral estimates $\{B_m\}$ in (15) over all m, we find (appendix A)

$$\sum_{m=0}^{N_2-1} B_m = N_1\ N_2\ K\ L_1\ w_o^{(d)}\ P_T\ , \tag{19}$$

where P_T is the sample power of the total data record:

$$P_T = \frac{1}{T} \sum_{n=0}^{T-1} |x_n|^2\ . \tag{20}$$

Thus if we adopt the reasonable rule to maintain the total sample power, we should scale all the $\{B_m\}$ by the factor $\left(N_1\ N_2\ K\ L_1\ w_o^{(d)}\right)^{-1}$; this feature is incorporated in the program listings here.

LAG WEIGHTINGS

A class of lag weightings that encompasses a broad and useful selection, including the rectangular, Hanning, Hamming, Blackman [3], Harris [19], and Nuttall [18] windows, is given by the form

$$w_n = \sum_{k=0}^{3} \alpha_k \cos(\pi nk/L_2) \quad \text{for } |n| \le L_2\ . \tag{21}$$

The particular example we will concentrate on here is the C1 window in [18, figure 12], where C1 denotes continuous first derivative, and

$$\{\alpha_k\}_0^3 = .355768,\ .487396,\ .144232,\ .012604\ . \tag{22}$$

Since the lag weighting appears linearly in the correlation domain, (see (12)-(14)), the power response of the window is directly proportional to the Fourier transform of (21), and not its square. Thus, as noted in [18, (18) and footnote], the sidelobe level is half that depicted in [18, figure 12]; namely, we have

$$\text{-46.66 dB peak sidelobes,} \quad \text{9 dB/octave decay.} \tag{23}$$

Other examples are available in [18] and can be used if deeper sidelobes or faster decay rates are required; however, the main lobe width must also be considered in these tradeoffs.

CHOICE OF PARAMETERS

In this section, we discuss some of the considerations that go into the selection of L_1, L_2, N_1, and N_2. We find that there is no absolute optimum, but there are useful guidelines to observe in order to minimize the fluctuations and execution time.

STABILITY OF FIRST-STAGE CORRELATION ESTIMATES

Because of the sectioning of the total of T data points into K abutting pieces, each of length L_1, first-stage correlation estimates $\{a_n\}$ in (10) employ

$$\begin{aligned} K\,L_1 &= T && \text{data points for zero delay;} \\ K\,(L_1-1) &= T-K && \text{data points for unit delay;} \\ K\,(L_1-n) &= T-n\,K && \text{data points for delay } n. \end{aligned} \tag{24}$$

This consideration alone would say that to minimize the loss of stability, choose K small, i.e., segment length L_1 large. However, since lag weighting (12)-(14) will only use delays up through L_2, the loss in stability will be relatively insignificant if $L_2 < L_1/2$, approximately; see [1, page 49, figure 15B] for specific quantitative results. For example, the stability for window C1, as measured in terms of quality ratio (2)-(3), deteriorates by about 9 percent at $L_2/L_1 = 1/2$, compared to the absolute optimum. Thus we will impose the limitation

$$L_1 \geq 2\ L_2(\max)\ , \tag{25}$$

where lag weighting length $L_2(\max)$ corresponds to the narrowest frequency resolution of interest, in order to hold random fluctuations at an acceptably low level.

SELECTION OF N_1

We have already seen in (11) and figure 3 that we must have $N_1 \geq L_1 + L_2$, in order to avoid wrap-around. However, there is no need for picking N_1 larger, since the FFTs of size N_1 are used only as a computing shortcut to getting the desired correlation of the averaged L_1-long data segments, which are then used for lag weighting. The N_1-point forward and inverse FFTs in (6) and (10) have no spectral spacing requirements whatsoever, nor do they affect the stability of the final spectral estimates $\{B_m\}$ in (15). Thus we will be interested in choosing N_1 as small as possible, subject to both limitations (11) and (25); this will also reduce storage and increase the speed of execution for each of these FFTs.

EXECUTION TIME

The time required to execute one full-precision N_1-point FFT on the Hewlett-Packard 9000 Model 520 computer has been determined empirically as

$$N_1 \ (.14 \ \ln N_1 + .396) \quad \text{msec} \tag{26}$$

to a high degree of accuracy, over the range $N_1 = 2^6 = 64$ to $N_1 = 2^{14} = 16384$. The particular constants in (26) will change for a different computer, but the general rule can be expected to hold quite well over this most useful range of values of N_1.

The total time to execute all the K first-stage FFTs in (6) and the single inverse FFT in (10) is then

$$(K+1) \ N_1 \ (.14 \ \ln N_1 + .396) \quad \text{msec.} \tag{27}$$

To minimize (27), we should make N_1 and K small. Since, from (4), $T = K \ L_1$, and since we want to use all available T data points, we should make L_1 large. However, we are subject to the limitation (11), $L_1 + L_2 \leq N_1$ (in order to avoid wrap-around), and we are interested in keeping N_1 small also, as noted above, in addition to being a power of 2.

A reasonable procedure for meeting these constraints and conflicting requirements is as follows: for given data length T and maximum lag length $L_2(\max)$ of interest, choose starter value

$$L_1 = 2\, L_2(\max) \quad \text{(for good stability)}. \tag{28}$$

Then take the smallest integer n satisfying the constraint

$$N_1 = 2^n \geq L_1 + L_2(\max) \quad \text{(to avoid wrap-around)}. \tag{29}$$

Then choose the largest L_1 satisfying

$$L_1 \leq N_1 - L_2(\max) \tag{30}$$

and a corresponding K such that equality

$$K\, L_1 = T \quad \text{(to use all the data)} \tag{31}$$

is met (or approximately met).

An example is informative at this point. Suppose T = 10,000 and we want $L_2(\max) = 250$. Then (28)-(30) yield, in order, $L_1 = 500$, $N_1 = 1024$, $L_1 \leq 774$. Then if we take $L_1 = 774$, we must have K = 12, yielding $K\, L_1 = 9288$, which is significantly below the allowed value 10,000 for this example. However, if we take $L_1 = 769$, then K = 13 yields $K\, L_1 = 9997$, which means

discarding only 3 of the available 10,000 data points. Thus a little juggling of the value of L_1 between the limits given by (28) and (30), coupled with the desire of meeting (31) as closely as possible (but not exceeding T), is recommended.

This procedure, (28)-(31), minimizes execution time (27) and realizes near-optimum stability of the spectral estimate. However, the particular choices are not critical. For example, if we instead took $L_1 = 714$ and $K = 14$ above, we get $K\ L_1 = 9996$, and the execution time (27) increases above that for $K = 13$ by the factor $(14+1)/(13+1) = 1.071$, while the stability degrades very slightly; see [1, figure 15B].

DIRECT CALCULATION OF CORRELATION

For T available data points, the number of multiplies and adds required to directly estimate the correlation at delays 0 and L_2 are T and $T - L_2$, respectively. Therefore a total of

$$\left(T - \frac{L_2}{2}\right)\left(L_2 + 1\right) \tag{32}$$

multiplies and adds are required for all delays in the range $[0, L_2]$. For the example above of $T = 10{,}000$, $L_2 = 250$, this is 2.5E6 operations. This direct approach takes 70 seconds on the Hewlett-Packard 9000 Model 520 computer, versus 20 seconds via the FFT approach presented above. Thus the advantage of employing the FFT technique is a significant reduction in execution time.

SIMULATION RESULTS

The results in this section are based on the two program listings in appendix B for complex and real data, respectively. An explanation of their use is given at the beginning of that appendix.

SINGLE TONE, NOISE FREE

The first example is a noise-free pure complex tone at zero frequency, with Δ_t = 1 second, T = 10,000 data points, L_1 = 769, K = 13 pieces, N_1 = 1024, and the C1 weighting given in (21)-(23). The resulting spectral estimate for L_2 = 250, N_2 = 16384, obtained via the programs* in appendix B, is given in figures 4 and 5, for frequencies $f_m = m/N_2$ in the range $[0, 8/L_2]$; the first null is at frequency $4/(2L_2) = 2/L_2$. (Compare this spectrum with the ideal result in [18, figure 12].) The difference in figures 4 and 5 is that the dB measure

$$10 \log |B_m| \tag{33}$$

---

*Observe that constraints (11), (17), and (28)-(31) have been observed, both in this example and in the programs.

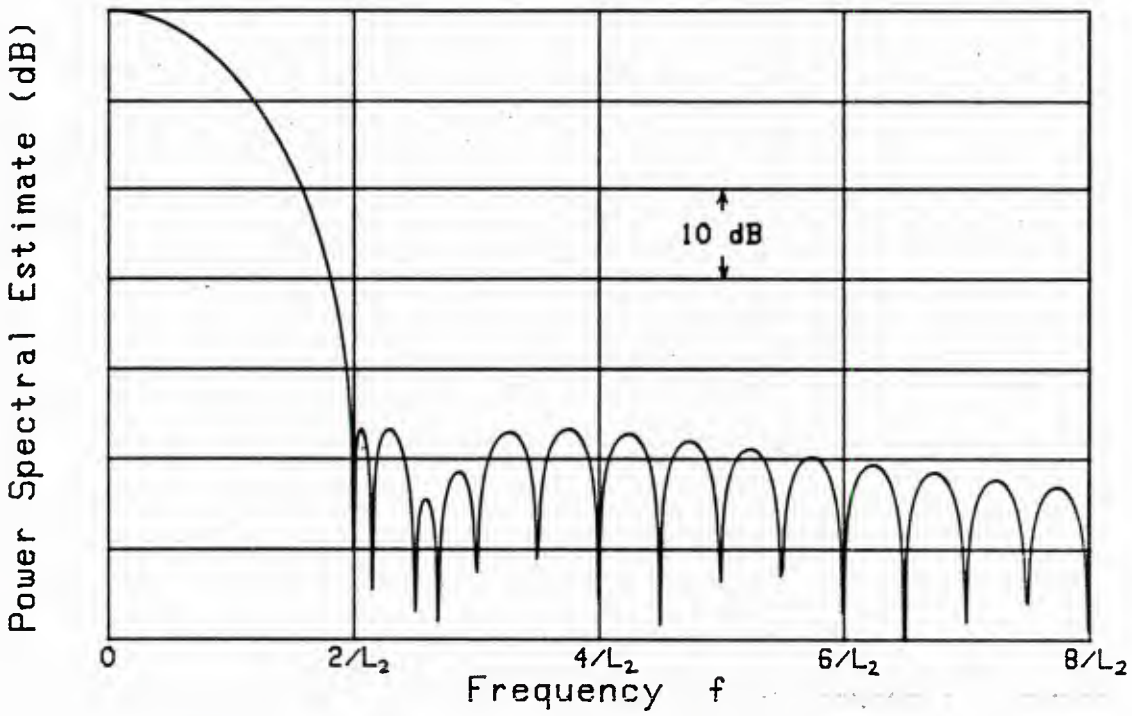

Figure 4. Pure Tone Analysis for $N_2 = 16384$; Negative Lobes Also

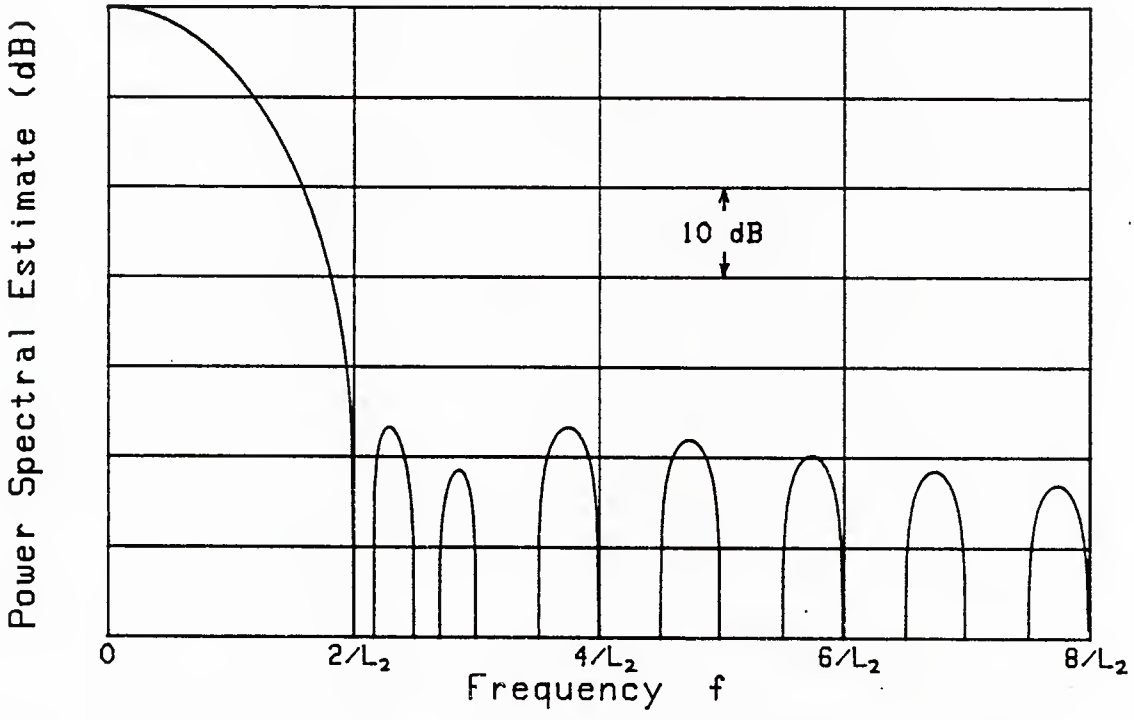

Figure 5. Pure Tone Analysis for $N_2 = 16384$; Positive Lobes Only

is plotted on the ordinate in figure 4, whereas the negative lobes ($B_m<0$) are not plotted in figure 5. The latter procedure, not (33), is the correct one and is adopted henceforth. The reason for the negative lobes in the spectral estimate is that the lag weighting and lag window appear linearly, not quadratically, in the equations; see (22) et seq. and [1, (50)-(51), (97)-(100)]. The presence of negative spectral estimates for some frequencies, i.e., $B_m < 0$ for some m, can actually be useful as an indicator of the presence of strong narrowband components, as noted by Blackman and Tukey [3, pages 13, 92, 115]. Of course, the addition of noise would fill in the deep valleys in figures 4 and 5.

The danger of using too small a value of N_2 for the second-stage FFT is depicted in figures 6 and 7 for N_2 = 1024 and 512, respectively. The only difference in figures 5, 6, and 7 is the value of N_2;(generally, any parameters not mentioned are maintained at the same values as for the previous figure). The frequency spacing, (16), becomes progressively coarser, to the point that the linear interpolation between frequency components (15), employed in all the figures, can lead to some questionable conclusions; hence we should observe requirement (17) on N_2. Since only one FFT of size N_2 need be performed, for each choice of lag length L_2, this is not a severe computational load; the bulk of the first-stage processing, using several small-size (N_1) FFTs is done only once and saved for as many second-stage spectral estimates of different resolutions as desired. Of course, for the coarser frequency resolutions, L_2 is smaller, thereby alleviating the requirement (17) on N_2.

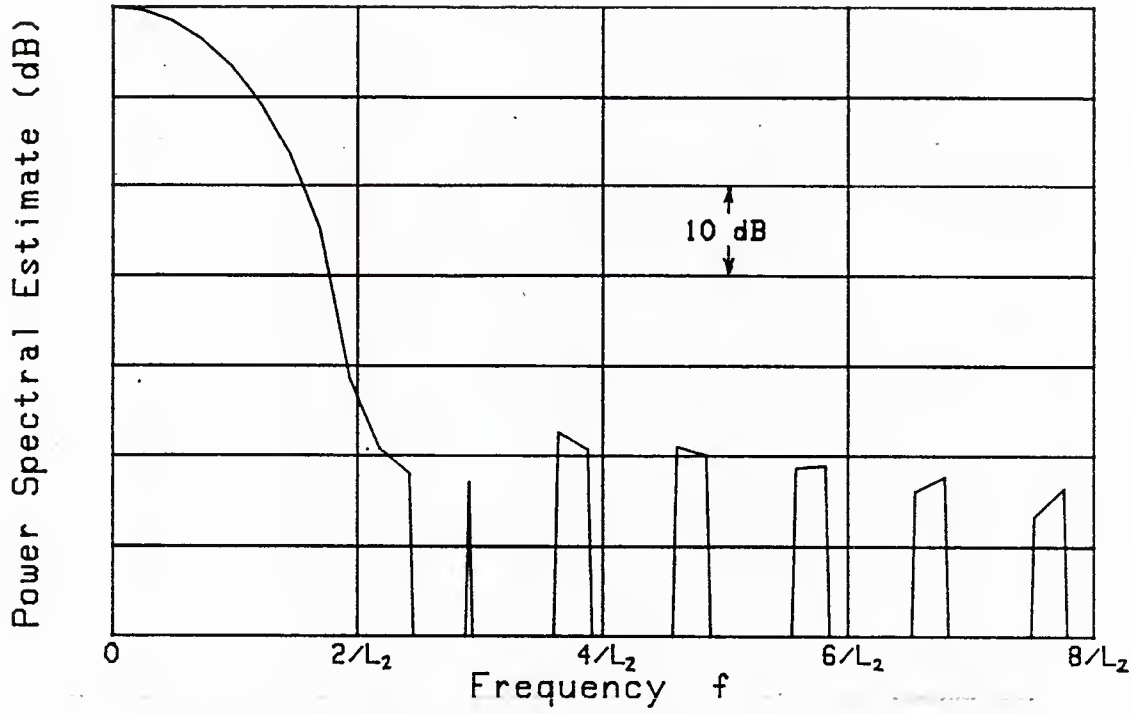

Figure 6. Pure Tone Analysis for $N_2 = 1024$

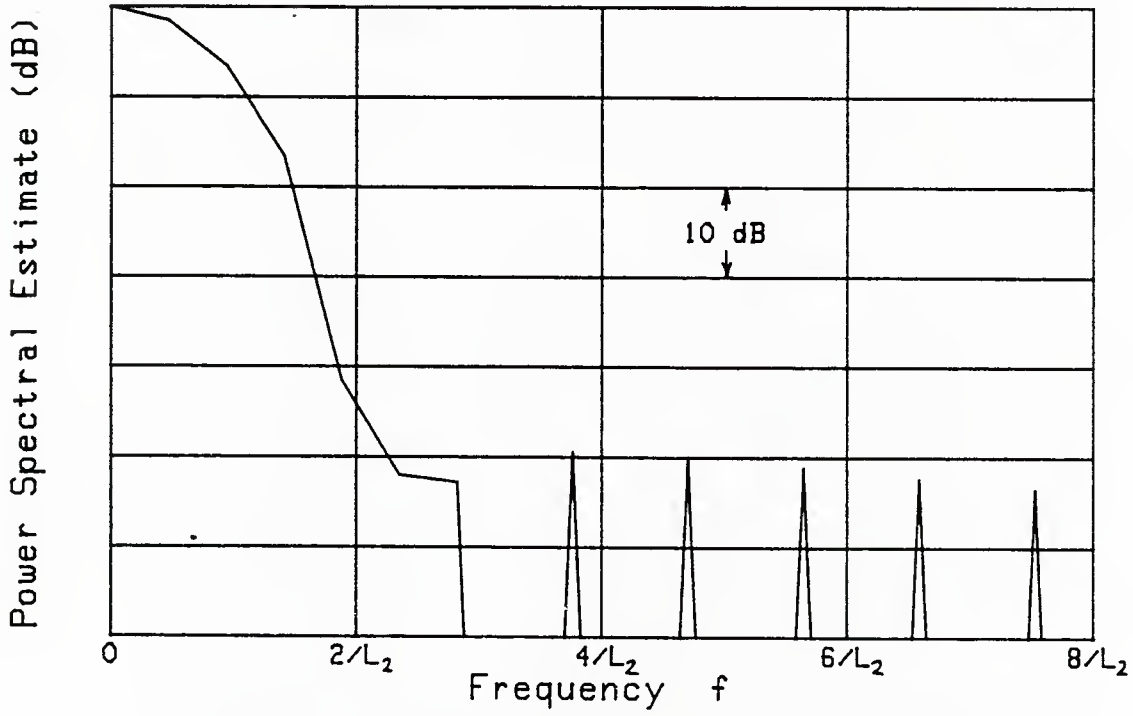

Figure 7. Pure Tone Analysis for $N_2 = 512$

Since there is no additive noise in this particular example, there is really no need to observe constraint (28) here. If we keep L_2 fixed at 250, we can decrease L_1, still subject to (12)-(14), and also decrease N_1, subject to (11), and realize the same spectral estimate as in figure 5. An example for $L_1 = 256$, $K = 39$, $K\,L_1 = 9984$, $N_1 = 512$, $N_2 = 16384$, yielded a result indistinguishable from figure 5, and is not plotted here. This confirms the earlier conclusion that the effective window depends only on the desirable weighting $\{w_n^{(d)}\}$ in (13)-(14), and not on the particular choices of L_1, K, N_1.

In figure 8, the frequency of the pure tone is changed from zero to 1/4 Hz, and the entire spectral estimate over frequency range (- 1/2, 1/2) Hz is plotted, with N_2 returned to value 16384. The rapid decay and deep sidelobes, (23), associated with the C1 weighting in (21)-(22) are quite evident. The darkened portion of the plot is caused by the detailed sidelobe structure of the C1 window.

On the other hand, if we simply eliminate the division of the first-stage correlation estimates by the autocorrelation of the temporal weighting, i.e., eliminate the triangular $1 - n/L_1$ term in (13) and (14), then the spectral estimate in figure 9 is obtained. Despite the retention of the desirable weighting in (13) and (14), there is a significant fill-in of the deep valleys and a less rapid decay of the estimate in figure 9.

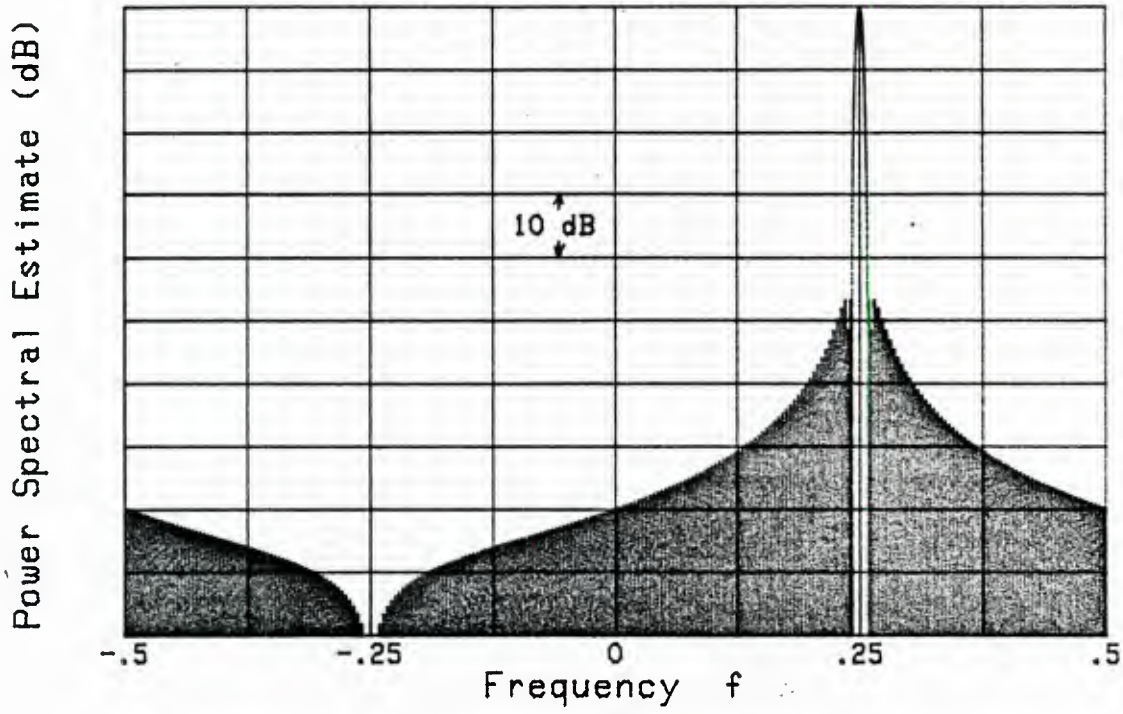

Figure 8. Pure Tone at Frequency .25 Hz; Lag-Reshaping

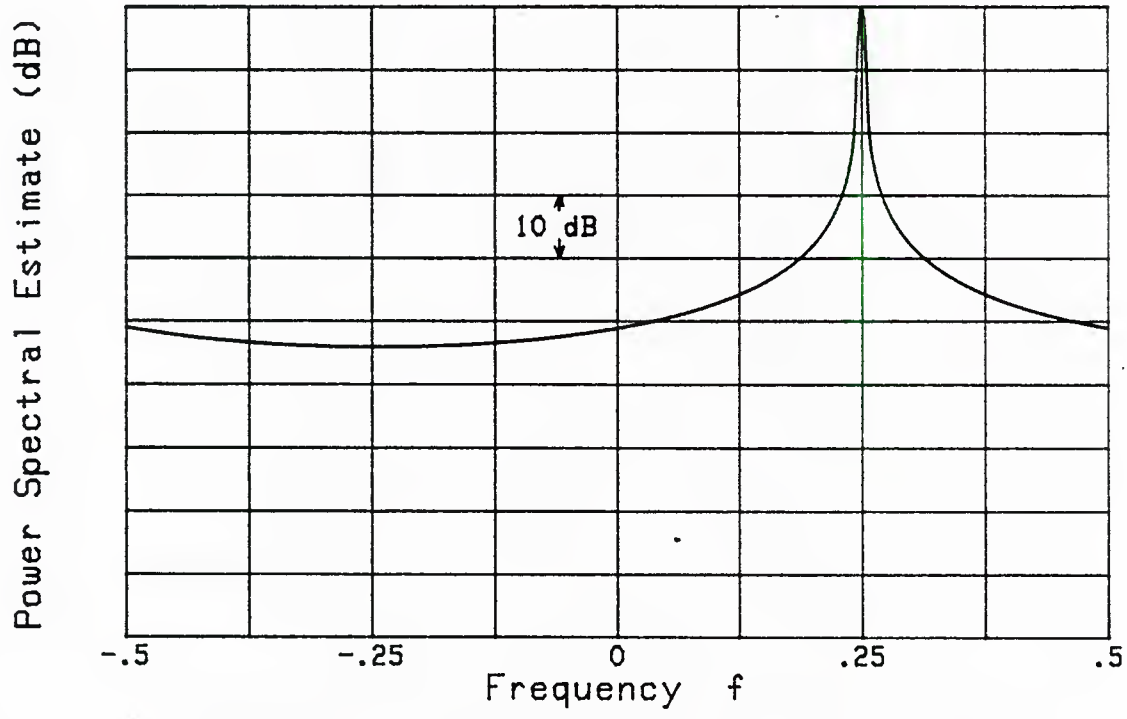

Figure 9. Pure Tone at Frequency .25 Hz; No Lag-Reshaping

TWO SEPARATED TONES IN WHITE NOISE

A similar comparison of the effect due to lack of lag-reshaping, i.e., removal of division by $1 - n/L_1$, is displayed in figures 10 and 11 for two well-separated pure tones plus white noise. The strong tone at frequency .25 Hz has a power level 47.8 dB stronger than the total white noise power, while the weak tone at frequency .0625 Hz (indicated by an arrow) has a power level -12.2 dB relative to the noise. Thus the ratio of signal powers is 60 dB. Whereas there is an indication of the weak tone in figure 10, at the correct level, there is none in figure 11, because of the poor sidelobe structure in the latter procedure. In fact, the sidelobes dominate the noise spectrum completely in figure 11.

In figures 12 and 13, the exact procedures are repeated for the same parameter values, except that the data are restricted to be real and the spectrum is only plotted over frequency range (0, 1/2) Hz. (The second program listing in appendix B, for real data, was employed for these two figures.) Again, the weak signal is indicated only for the case of lag-reshaping in figure 12.

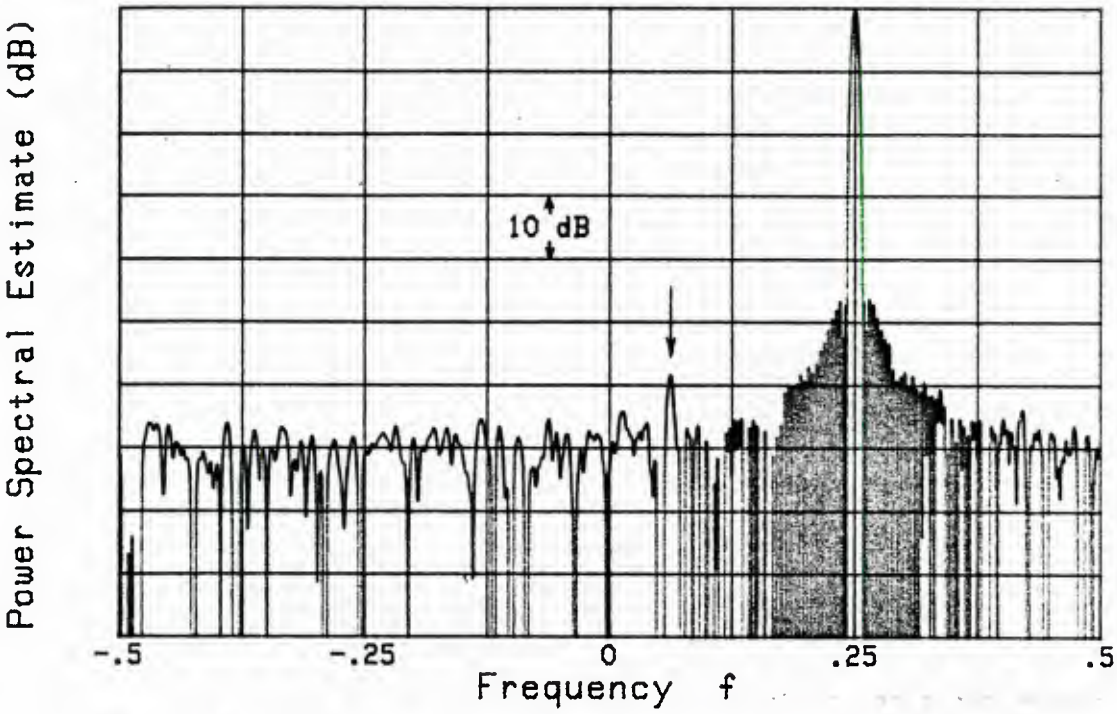

Figure 10. Two Complex Tones plus White Noise; Lag-Reshaping

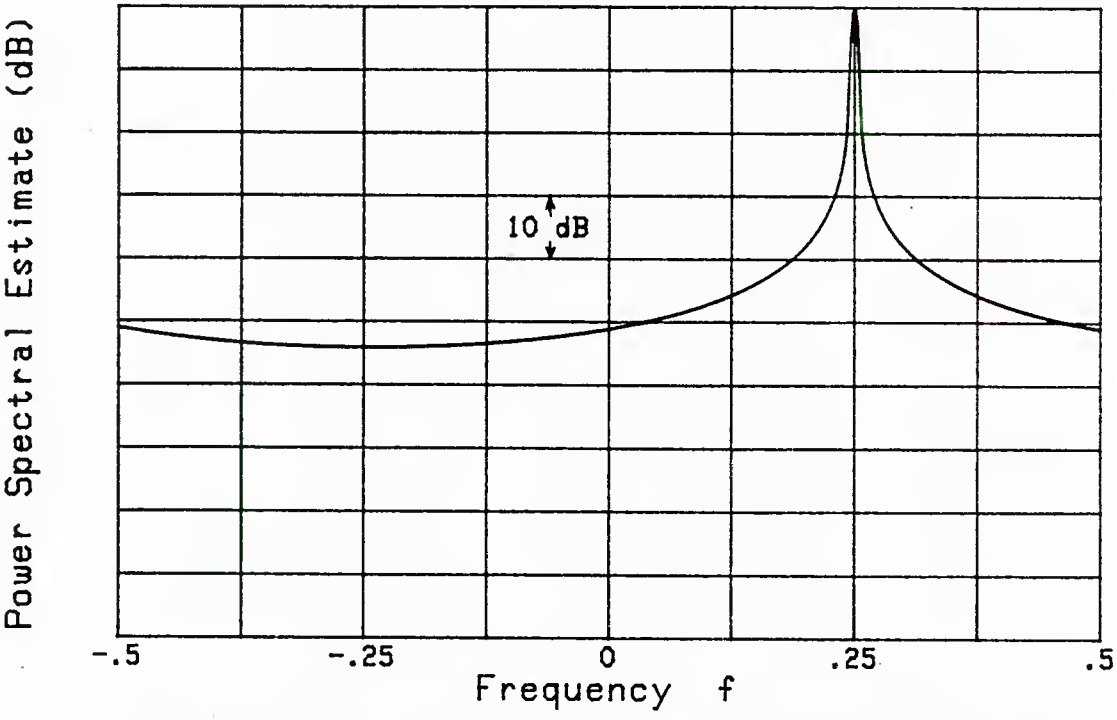

Figure 11. Two Complex Tones plus White Noise; No Lag-Reshaping

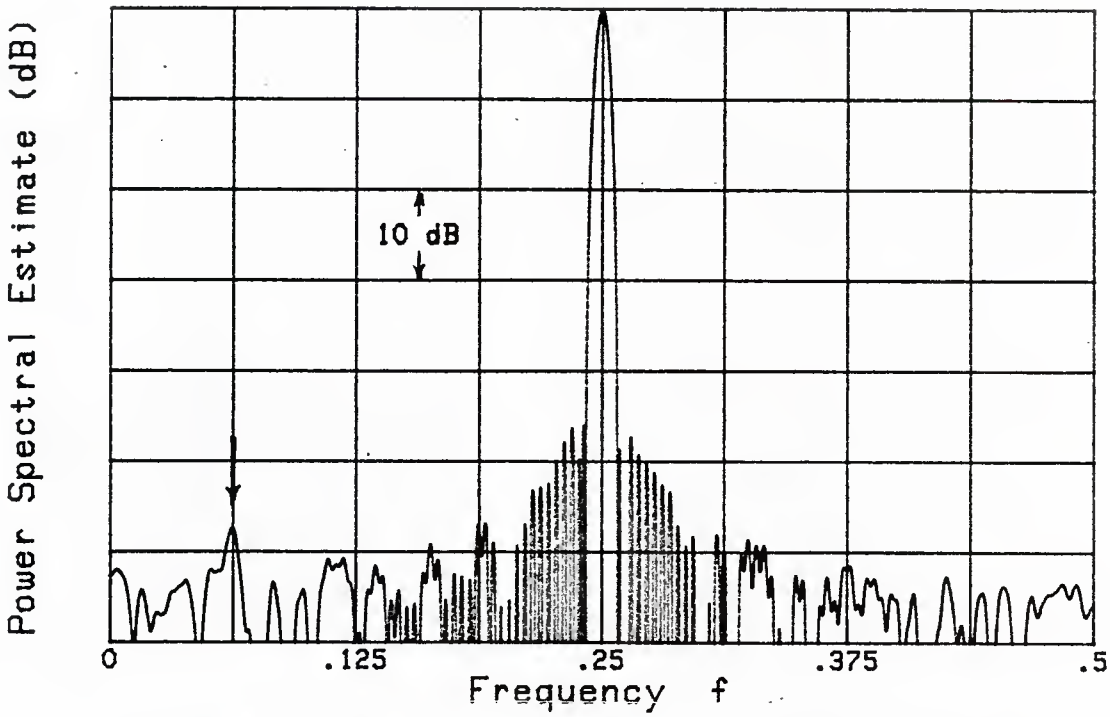

Figure 12. Two Real Tones plus White Noise; Lag-Reshaping

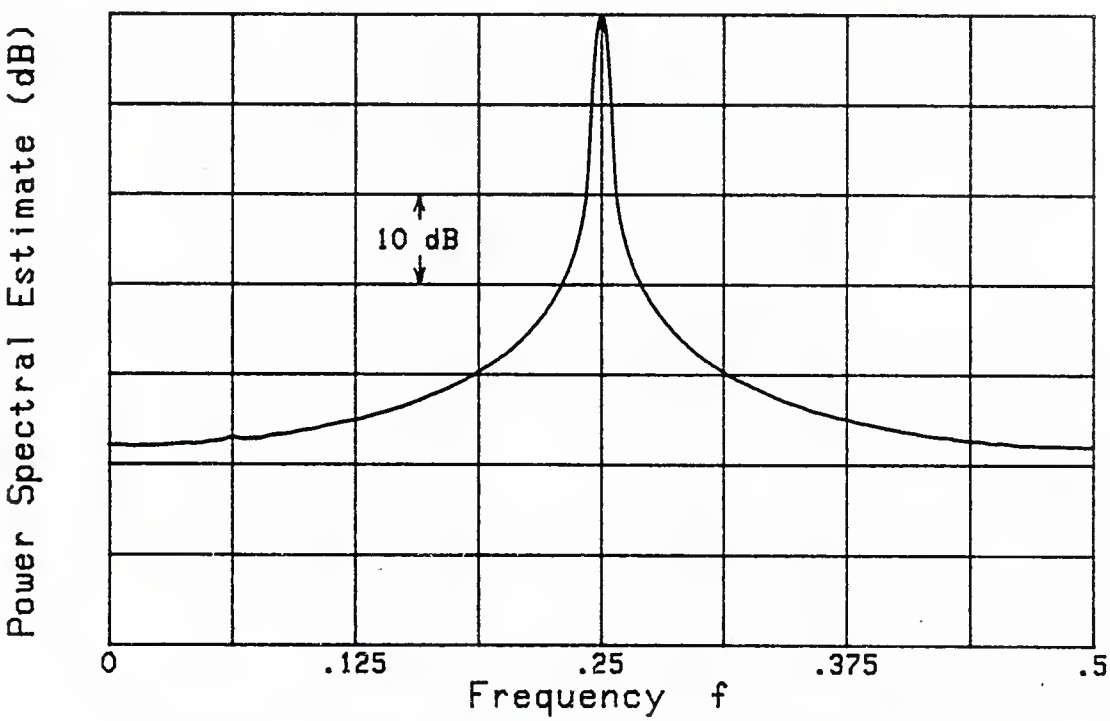

Figure 13. Two Real Tones plus White Noise; No Lag-Reshaping

TWO CLOSE TONES IN WHITE NOISE

In figures 14 and 15, a strong complex tone at frequency .25 Hz has a power level 17.8 dB stronger than the total white noise power, while the weak tone at frequency .265 Hz has a power level of -12.2 dB relative to the noise. Thus the ratio of signal powers is 30 dB. Whereas the lag-reshaping spectral estimate in figure 14 succeeds in resolving the two close tones at frequency separation .015 Hz, the result in figure 15, for no lag-reshaping, indicates only one of the tonals. It may be observed that the detailed wiggles in the two spectral estimates are virtually identical, except for frequencies near the tone locations.

Finally, in figures 16 and 17, the effect of decreasing lag weighting length L_2 is demonstrated. Specifically, figures 14, 16, 17 all employ lag-reshaping, the only difference in the three figures being that L_2 = 250, 200, 150, respectively. Whereas the weak close tonal is well-resolved in figure 14, it is lost in figure 17; the estimate in figure 16 is intermediate and on the border of being resolved. The familiar tradeoff of resolution versus stability is well demonstrated in figures 14, 16, 17. Namely, as the resolution degrades (mainlobe widens), the fluctuations in the spectral estimate decrease; figures 16 and 17 are progressively smoother versions of figure 14. Which case to prefer depends on the particular situation under investigation, including factors such as the proximity of tones with widely different strengths, and on the particular colored noise spectrum encountered. Quantitative evaluation of the stability is considered in the next section.

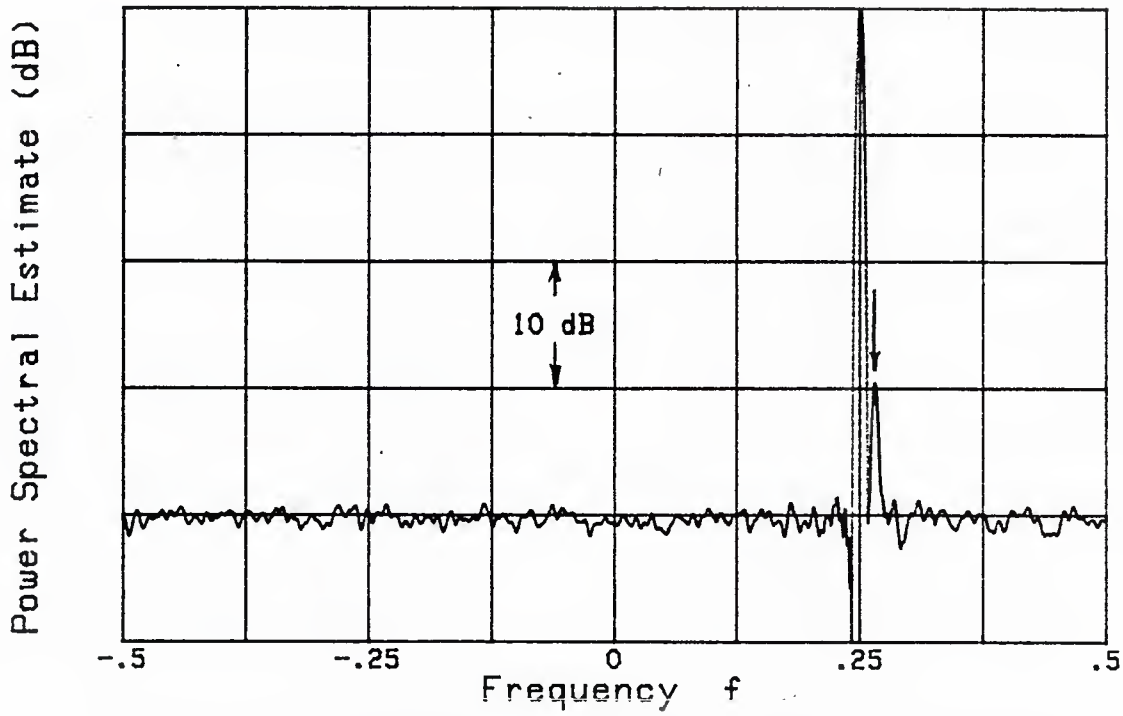

Figure 14. Two Close Tones plus White Noise; Lag-Reshaping, $L_2 = 250$

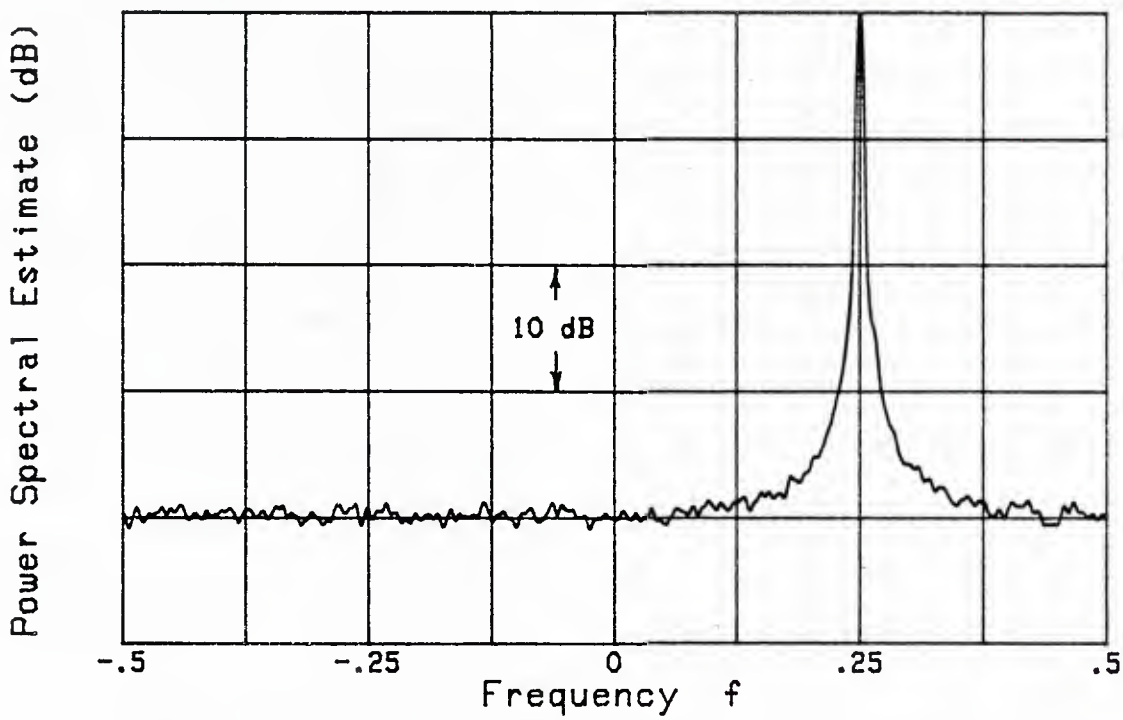

Figure 15. Two Close Tones plus White Noise; No Lag-Reshaping, $L_2 = 250$

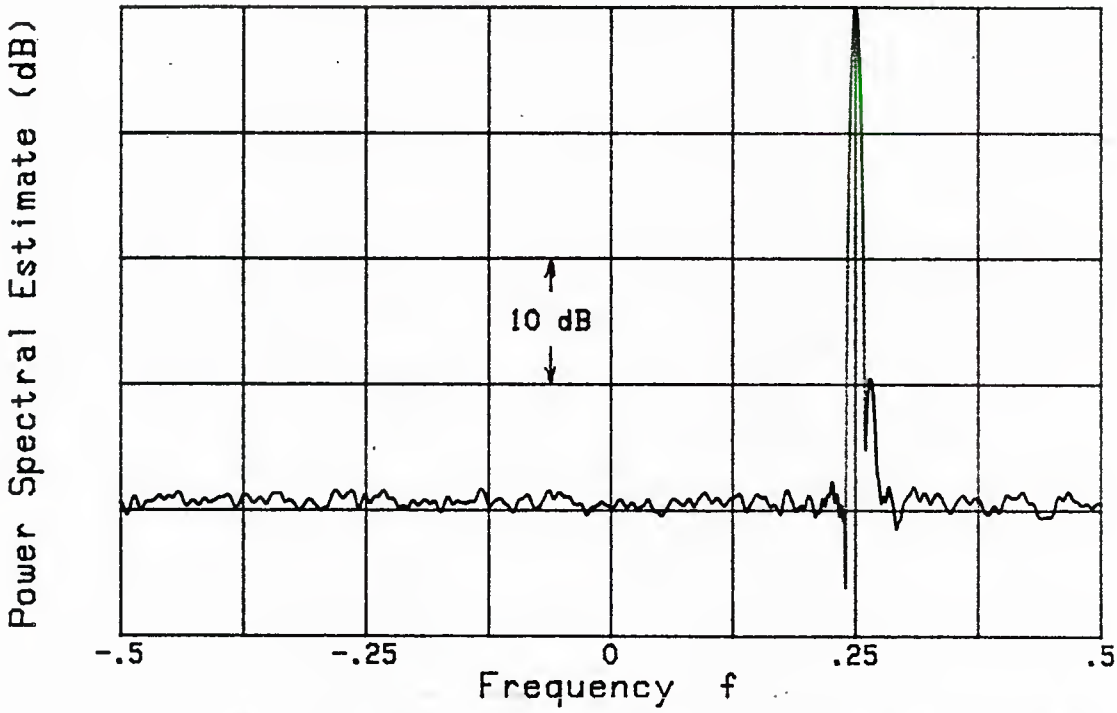

Figure 16. Two Close Tones plus White Noise; Lag-Reshaping, $L_2 = 200$

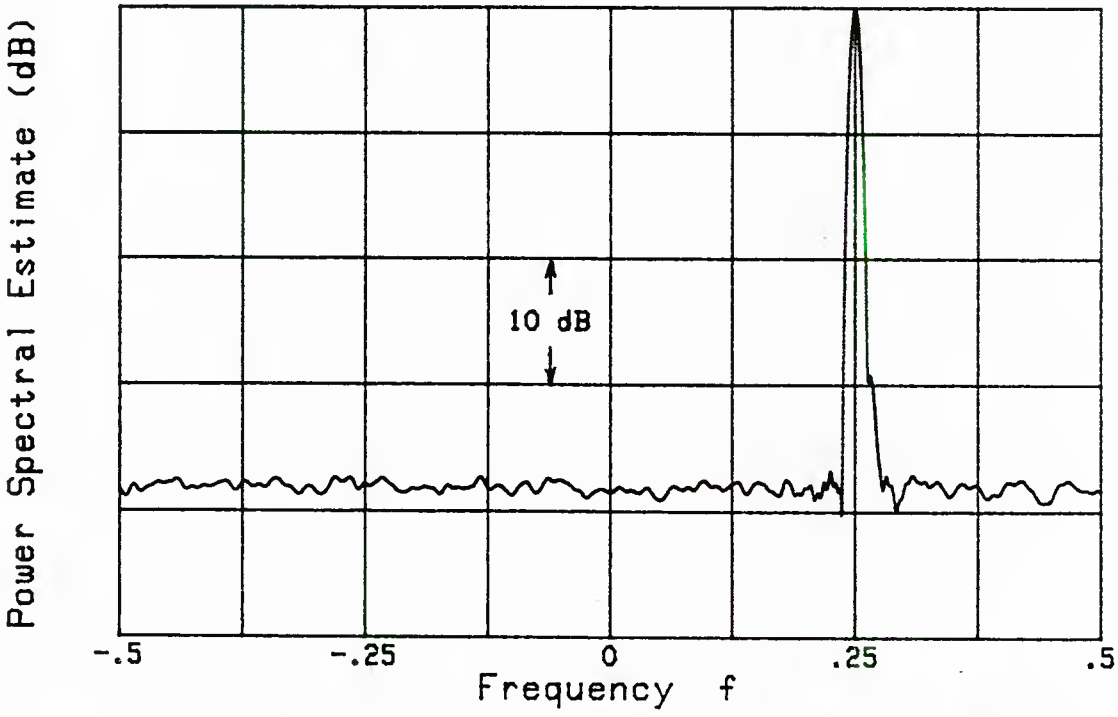

Figure 17. Two Close Tones plus White Noise; Lag-Reshaping, $L_2 = 150$

VARIANCE OF SPECTRAL ESTIMATE

THEORETICAL RESULTS

The variance of the spectral estimate obtained via the generalized technique including temporal and lag weighting was derived and evaluated in [1, pages 41-57]. In particular, for abutting rectangular temporal weighting, the NQR, defined in (2) et seq. above, is given by [1, (138)] as

$$\text{NQR} = \frac{\int_0^{L_2} d\tau\, w_d^2(\tau)\,(1 - \tau/L_1)^{-1}}{\int_0^{L_2} d\tau\, w_d^2(\tau)} = \frac{\int_0^{1} dx\, w_d^2(L_2 x)\,(1 - x\, L_2/L_1)^{-1}}{\int_0^{1} dx\, w_d^2(L_2 x)} \tag{34}$$

in the case of lag-reshaping, where $w_d(\tau)$ is the continuous analog of the discrete desirable weighting $w_n^{(d)}$ employed here in (13) and (14).

For the class of continuous weightings (compare (21))

$$w_d(\tau) = \sum_{k=0}^{3} \alpha_k \cos(\pi k \tau / L_2) \quad \text{for} \quad |\tau| < L_2 \,, \tag{35}$$

the NQR in (34) becomes

$$\text{NQR} = \frac{\int_0^{1} dx \left(\sum_{k=0}^{3} \alpha_k \cos(\pi k x) \right)^2 (1 - x\, L_2/L_1)^{-1}}{\int_0^{1} dx \left(\sum_{k=0}^{3} \alpha_k \cos(\pi k x) \right)^2} \,, \tag{36}$$

which depends only on the ratio L_2/L_1 and coefficients $\{\alpha_k\}$. This quantity was plotted in [1, page 49, figure 15B] for various windows. The special case of the C1 window, (22), is replotted here in figures 18 and 19 as the solid curve.

SIMULATION RESULTS

In order to corroborate these theoretical results, white Gaussian noise was generated for 25 independent trials, each of length T = 10000 samples. The data were spectral analyzed for lag length L_2 = 1000 and for a variety of temporal lengths L_1. The results for the NQR, determined by using <u>all</u> frequency bins on all the trials, are shown as crosses in figure 18. The optimum quality ratio, as given by (3), is

$$Q = \frac{1}{TB_e} = \frac{2\ L_2\ c\{w_d\}}{T} = \frac{2 * 1000 * .2558}{10000} = .0512\ , \qquad (37)$$

where we employed [1, (11), (101), and Table 1]. Keeping L_2 fixed is tantamount to holding the frequency resolution constant, while varying L_1 corresponds to different segment lengths (all subject to $L_1 > L_2$, of course).

Results for L_2 = 250 are plotted in figure 19, based now on at least 100 trials for each value of L_1 considered; now the optimum Q = .0128. The simulation results for white Gaussian noise slightly overestimate the theoretical results in figure 19, whereas the converse is true in figure 18. Also added in figure 19 are simulation results for white input data which are not Gaussian, but rather have a flat probability density function over their

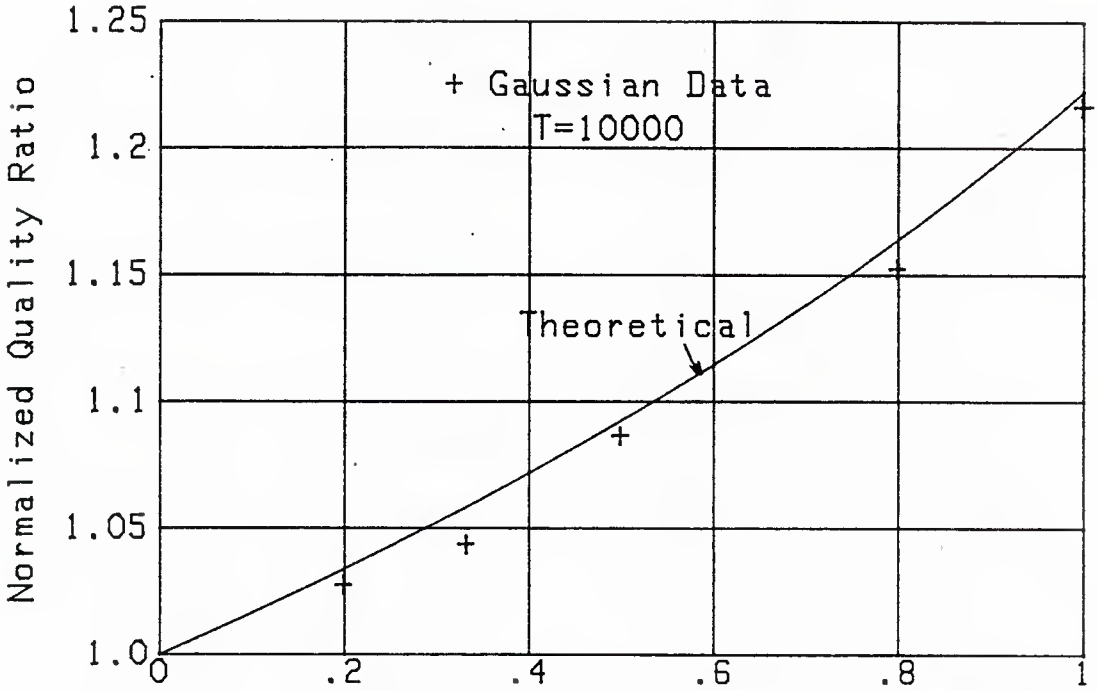

Figure 18. NQR for L_2=1000 and Window C1

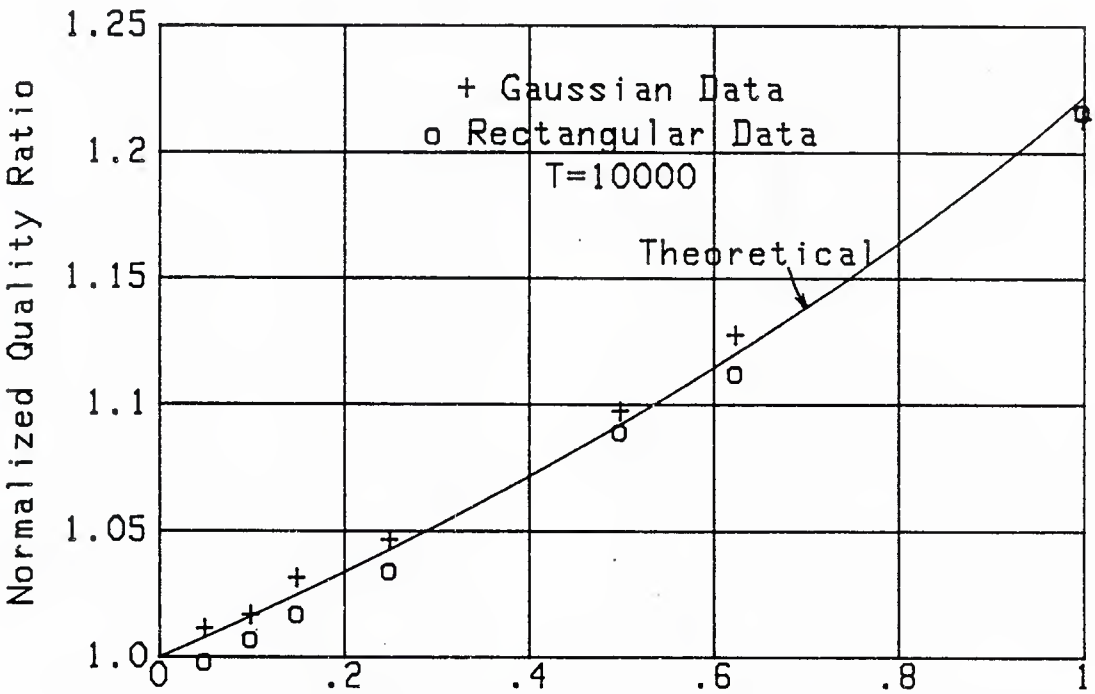

Figure 19. NQR for L_2=250 and Window C1

nonzero extent; see the circles, labeled "rectangular data," in figure 19. The discrepancy between the theoretical results for Gaussian data and the simulation results for rectangular data is believed to be real (although it is only approximately a 2 percent difference), because these results were based on 500 trials for each value of L_1. In any event, the theoretical results predict the stability very well, over the full range of L_2/L_1. At $L_2/L_1 = .5$, for example, the loss in stability is only about 8 to 9 percent, as measured by the quality ratio (2).

APPROXIMATION TO NQR

For small L_2/L_1, the NQR in (34) behaves approximately as

$$\text{NQR} \cong \frac{I_0 + I_1 (L_2/L_1) + I_2 (L_2/L_1)^2 + I_3 (L_2/L_1)^3}{I_0} , \tag{38}$$

where we define the dimensionless constants

$$I_n = \int_0^1 dx \; w_d^2(L_2 x) \; x^n \quad \text{for} \quad n = 0, 1, 2, 3 . \tag{39}$$

For the class of continuous weightings specified in (35), there follows

$$\begin{aligned} I_0 &= \alpha_0^2 + \tfrac{1}{2} (\alpha_1^2 + \alpha_2^2 + \alpha_3^2) , \\ I_1 &= \tfrac{1}{2} I_0 - \frac{4}{\pi^2} T_1 , \\ I_2 &= \tfrac{1}{3} I_0 + \frac{1}{4\pi^2} (\alpha_1^2 + \tfrac{1}{4} \alpha_2^2 + \tfrac{1}{9} \alpha_3^2) - \frac{4}{\pi^2} T_2 , \end{aligned} \tag{40}$$

where

$$T_1 = \alpha_0 \alpha_1 + \frac{1}{9} \alpha_0 \alpha_3 + \frac{5}{9} \alpha_1 \alpha_2 + \frac{13}{25} \alpha_2 \alpha_3 ,$$

$$T_2 = T_1 - \frac{1}{4} \alpha_0 \alpha_2 - \frac{5}{32} \alpha_1 \alpha_3 . \qquad (41)$$

Equations (38)-(41) enable a simple approximate calculation of the NQR for any weighting in class (35).

When applied to the C1, C3, C5 windows in [18, figures 10, 11, 12], the numerical results for $\left\{I_n/I_0\right\}_1^3$ are, respectively,

.16114,	.04036,	.01273	for window	C1;
.15362,	.03664,	.01100	for window	C3;
.14168,	.03111,	.00859	for window	C5. (42)

Substitution in (38) yields results which agree very well with figures 18 and 19 and, more generally, with [1, figure 15B].

SUMMARY

Programs for spectral estimation of complex data as well as real data have been given and exercised under a wide range of parameter choices. They allow the data to be generated or made available in abutting blocks of L_1 data points at a time, and they employ no temporal weighting at all. The user must replace subroutine SUB Data by his own data input routine. The subroutine SUB Fft14z listed in appendix B employs zero-subscripted arrays, as encountered directly in the equations, and can handle sizes up to $2^{14} = 16384$.

The benefits to be accrued from lag-reshaping have been demonstrated by simulation, for a variety of situations including multiple tones in noise. The ability to obtain several spectral estimates with different frequency resolutions has been incorporated in the programs in such a way that the bulk of the first-stage spectral estimates do not have to be recalculated. This enables the user to make his own decisions on resolution versus stability, without having to do extensive computations repeatedly.

Reverse Blank

APPENDIX A. SUM OF POWER SPECTRAL ESTIMATES

The power spectral estimate B_m is given by (15) for $0 \le m \le N_2 - 1$. The sum over all m is

$$\sum_{m=0}^{N_2-1} B_m = N_2\, b_o = N_2\, w_o^{(d)}\, a_o =$$

$$= N_2\, w_o^{(d)} \sum_{m=0}^{N_1-1} A_m = N_2\, w_o^{(d)} \sum_{m=0}^{N_1-1} \sum_{k=1}^{K} \left| X_m^{(k)} \right|^2 =$$

$$= N_2\, w_o^{(d)} \sum_{k=1}^{K} \sum_{m=0}^{N_1-1} \left| X_m^{(k)} \right|^2 = N_2\, w_o^{(d)} \sum_{k=1}^{K} N_1 \sum_{n=0}^{L_1-1} \left| x_n^{(k)} \right|^2 =$$

$$= N_1\, N_2\, w_o^{(d)} \sum_{n=0}^{T-1} \left| x_n \right|^2 , \qquad \text{(A-1)}$$

by use of (14), (10), (9), (6), (5), (4), in order. In terms of the sample power of the total data record,

$$P_T = \frac{1}{T} \sum_{n=0}^{T-1} \left| x_n \right|^2 , \qquad \text{(A-2)}$$

the sum in (A-1) becomes

$$\sum_{m=0}^{N_2-1} B_m = N_1\, N_2\, K\, L_1\, w_o^{(d)}\, P_T . \qquad \text{(A-3)}$$

Reverse Blank

APPENDIX B. PROGRAMS FOR LAG-RESHAPING SPECTRAL ANALYSIS

There are two main programs in this appendix, written for the Hewlett-Packard 9000 Model 520 computer. The first is for complex data, while the latter accommodates only real data. The following explanation is keyed to the complex data program, but applies directly to the real data program as well.

Input parameters T, L_1, L_2(max), N_1 are required at the top of the program in lines 20-50. The lag weighting coefficients of interest are entered in line 60. Constraint (29) is enforced in lines 100-130. The number of pieces, K, and the number of data points used, K L_1, are computed in lines 160 and 180. The input data are entered via SUB Data in line 280, L_1 data points at a time; that is, data values $\left\{x_n^{(k)}\right\}$ for $0 \leq n \leq L_1 - 1$, as given by (5), are accessed by the CALL in line 280 with arguments Ks, L1 (= piece k, segment length L_1). Division by the autocorrelation of the temporal weighting is accomplished once, in loop 380-420.

At this point, the first-stage calculations are complete; the correlation domain quantities are stored in arrays Xa, Ya. Input parameters L_2, N_2 must now be entered in lines 440, 450. Constraints (14) and (11) are enforced in lines 460-510. The lag weighting is applied in loop 620-680, taking figure 3 into account, while the scaling considerations of (19)-(20) imply line 730.

Finally, the spectral estimate is plotted in dB over the frequency range (-1/2, 1/2) Hz in lines 770-860. (For real data, the spectrum is only plotted over the range (0, 1/2) Hz, since it is symmetric about the origin.)

The FFT subroutine in lines 900 - 1710 uses zero-subscripted arrays, just as encountered in the usual mathematical definition; it can handle FFT sizes up to $2^{14} = 16384$. The subroutine SUB Data in lines 1730 - 1900 must be replaced by the user; however, notice should be taken of lines 1810 - 1830 and the storage locations in lines 1860 - 1870, in order to ensure that L_1 data points at a time are properly stored in locations 0 through $L_1 - 1$.

```
 10  ! LAG RE-SHAPING SPECTRAL ANALYSIS FOR COMPLEX DATA
 20    T=10000                 !  TOTAL NUMBER OF DATA POINTS
 30    L1=769                  !  NUMBER OF DATA POINTS PER PIECE
 40    L2max=250               !  MAXIMUM LAG WEIGHTING LENGTH
 50    N1=1024                 !  SIZE OF FIRST-STAGE FFT N1>=L1+L2max
 60    DATA .355768,.487396,.144232,.012604   !  LAG WEIGHTING COEFFICIENTS
 70  ! TR 6239, page 16, figure 12: -46.66 dB sidelobes, 9 dB/octave decay
 80    DIM X(0:16383),Y(0:16383),Xa(0:8191),Ya(0:8191)
 90    DOUBLE T,L1,L2max,N1,N1m,K,Ks,Ns,L2,N2,N2m     !  INTEGERS
100    IF N1>=L1+L2max THEN 140
110    PRINT "N1 INCREASED, SO AS TO BE AT LEAST L1+L2max"
120    N1m=INT(LOG(L1+L2max)/LOG(2))+1
130    N1=2^N1m
140    N1m=N1-1
150    REDIM X(0:N1m),Y(0:N1m),Xa(0:N1m),Ya(0:N1m)
160    K=INT(T/L1)                      !  NUMBER OF DATA SEGMENTS
170    PRINT "T =";T;"   L1 =";L1;"   L2max =";L2max;"   N1 =";N1;"   K =";K
180    PRINT "USED";K*L1;"OF THE TOTAL NUMBER OF DATA POINTS,";T
190    READ A0,A1,A2,A3
200    A=1./(A0+A1+A2+A3)               !  NORMALIZE LAG WEIGHTS
210    A0=A0*A
220    A1=A1*A
230    A2=A2*A
240    A3=A3*A
250    MAT Xa=(0.)
260    MAT Ya=(0.)
270    FOR Ks=1 TO K
280    CALL Data(Ks,L1,X(*),Y(*))       !  L1 DATA POINTS AT A TIME
290    FOR Ns=L1 TO N1m
300    X(Ns)=Y(Ns)=0.
310    NEXT Ns
```

```
320     CALL Fft14z(N1,X(*),Y(*))       !  INTO FREQUENCY DOMAIN
330     FOR Ns=0 TO N1m
340     Xa(Ns)=Xa(Ns)+X(Ns)*X(Ns)+Y(Ns)*Y(Ns)  !  POWER AVERAGING
350     NEXT Ns
360     NEXT Ks
370     CALL Fft14z(N1,Xa(*),Ya(*))     !  INTO LAG DOMAIN
380     FOR Ns=0 TO L1-1
390     A=L1/(L1-Ns)
400     Xa(Ns)=Xa(Ns)*A                 !  DIVIDE BY CORRELATION
410     Ya(Ns)=-Ya(Ns)*A                !  OF TEMPORAL WEIGHTING
420     NEXT Ns
430     BEEP
440     INPUT "L2 =",L2         !  LAG WEIGHTING LENGTH L2<L1, L2<=N1-L1
450     INPUT "N2 =",N2         !  SIZE OF SECOND-STAGE FFT N2 (>L2*10 IS GOOD)
460     IF L2<L1 THEN 490
470     PRINT "L2 REDUCED TO L1-1, TO AVOID DIVISION BY ZERO"
480     L2=L1-1
490     IF L2<=L2max THEN 520
500     PRINT "L2 REDUCED TO L2max, TO AVOID WRAP-AROUND REGION"
510     L2=L2max
520     IF N2>L2+L2 THEN 560
530     PRINT "N2 INCREASED, SO AS TO BE GREATER THAN L2*2"
540     N2m=INT(LOG(L2+L2+1)/LOG(2))+1
550     N2=2^N2m
560     PRINT "L2 =";L2;"      N2 =";N2
570     N2m=N2-1
580     REDIM X(0:N2m),Y(0:N2m)
590     A=PI/L2
600     X(0)=Xa(0)
610     Y(0)=0.
620     FOR Ns=1 TO L2
630     B=Ns*A
640     W=A0+A1*COS(B)+A2*COS(B+B)+A3*COS(B+B+B)
650     X(Ns)=X(N2-Ns)=Xa(Ns)*W         !  LAG WEIGHTING
660     Y(Ns)=B=Ya(Ns)*W
670     Y(N2-Ns)=-B
680     NEXT Ns
690     FOR Ns=L2+1 TO N2m-L2
700     X(Ns)=Y(Ns)=0.
710     NEXT Ns
720     CALL Fft14z(N2,X(*),Y(*))       !  INTO FREQUENCY DOMAIN
730     MAT X=X/(FLT(K)*L1*N1*N2)
740     Big=MAX(X(*))
750     Db=LGT(Big)*10.
760     PRINT "Big =";Big;"      dB max =";Db
770     PLOTTER IS "GRAPHICS"
780     GRAPHICS ON
790     WINDOW -N2/2,N2/2,-70.,0.
800     GRID N2/8,10.
810     FOR Ns=-N2/2 TO N2/2
820     Ks=Ns MODULO N2
830     W=MAX(X(Ks),1.E-20)
840     PLOT Ns,LGT(W)*10.-Db
850     NEXT Ns
860     PENUP
870     GOTO 440
880     END
890     !
```

```
 900    SUB Fft14z(DOUBLE N,REAL X(*),Y(*)) ! . N=2^INTEGER<=2^14=16384; 0 SUBS
 910    DOUBLE N1,N2,N3,N4,Log2n,J,K        !  INTEGERS < 2^31 = 2,147,483,648
 920    DOUBLE I1,I2,I3,I4,I5,I6,I7,I8,I9,I10,I11,I12,I13,I14
 930    N1=N/4
 940    ALLOCATE C(0:N1),DOUBLE L(0:13)     !  QUARTER-COSINE TABLE IN C(*)
 950    A=(PI+PI)/N
 960    FOR J=0 TO N1
 970    C(J)=COS(A*J)
 980    NEXT J
 990    N2=N1+1
1000    N3=N2+1
1010    N4=N3+N1
1020    Log2n=1.4427*LOG(N)
1030    FOR I1=1 TO Log2n
1040    I2=2^(Log2n-I1)
1050    I3=I2+I2
1060    I4=N/I3
1070    FOR I5=1 TO I2
1080    I6=(I5-1)*I4+1
1090    IF I6<=N2 THEN 1130
1100    A1=-C(N4-I6-1)
1110    A2=-C(I6-N1-1)
1120    GOTO 1150
1130    A1=C(I6-1)
1140    A2=-C(N3-I6-1)
1150    FOR I7=0 TO N-I3 STEP I3
1160    I8=I7+I5-1
1170    I9=I8+I2
1180    A3=X(I8)-X(I9)
1190    A4=Y(I8)-Y(I9)
1200    X(I8)=X(I8)+X(I9)
1210    Y(I8)=Y(I8)+Y(I9)
1220    X(I9)=A1*A3-A2*A4
1230    Y(I9)=A1*A4+A2*A3
1240    NEXT I7
1250    NEXT I5
1260    NEXT I1
1270    I1=Log2n+1
1280    FOR I2=1 TO 14
1290    L(I2-1)=1
1300    IF I2>Log2n THEN 1320
1310    L(I2-1)=2^(I1-I2)
1320    NEXT I2
1330    K=0
1340    FOR I1=1 TO L(13)
1350    FOR I2=I1 TO L(12) STEP L(13)
1360    FOR I3=I2 TO L(11) STEP L(12)
1370    FOR I4=I3 TO L(10) STEP L(11)
1380    FOR I5=I4 TO L(9) STEP L(10)
1390    FOR I6=I5 TO L(8) STEP L(9)
1400    FOR I7=I6 TO L(7) STEP L(8)
1410    FOR I8=I7 TO L(6) STEP L(7)
1420    FOR I9=I8 TO L(5) STEP L(6)
1430    FOR I10=I9 TO L(4) STEP L(5)
1440    FOR I11=I10 TO L(3) STEP L(4)
1450    FOR I12=I11 TO L(2) STEP L(3)
1460    FOR I13=I12 TO L(1) STEP L(2)
1470    FOR I14=I13 TO L(0) STEP L(1)
```

```
1480    J=I14-1
1490    IF K>J THEN 1560
1500    A=X(K)
1510    X(K)=X(J)
1520    X(J)=A
1530    A=Y(K)
1540    Y(K)=Y(J)
1550    Y(J)=A
1560    K=K+1
1570    NEXT I14
1580    NEXT I13
1590    NEXT I12
1600    NEXT I11
1610    NEXT I10
1620    NEXT I9
1630    NEXT I8
1640    NEXT I7
1650    NEXT I6
1660    NEXT I5
1670    NEXT I4
1680    NEXT I3
1690    NEXT I2
1700    NEXT I1
1710    SUBEND
1720    !
1730    SUB Data(DOUBLE Ks,L1,REAL X(*),Y(*))
1740    DOUBLE J1,J2,J
1750    W1=2.*PI*.25            !  TONE FREQUENCY 1
1760    W2=2.*PI*.265           !  TONE FREQUENCY 2
1770    T1=.31                  !  TONE PHASE 1
1780    T2=.77                  !  TONE PHASE 2
1790    Db2=-30.                !  RELATIVE TONE STRENGTH
1800    A2=10.^(Db2/20.)
1810    J2=Ks*L1-1
1820    J1=J2-L1+1
1830    FOR J=J1 TO J2
1840    P1=W1*J+T1
1850    P2=W2*J+T2
1860    X(J-J1)=COS(P1)+A2*COS(P2)+(RND-.5)*.316
1870    Y(J-J1)=SIN(P1)+A2*SIN(P2)+(RND-.5)*.316
1880  ! (RND-.5)+i(RND-.5) has power 1/12+1/12 = -7.78 dB
1890    NEXT J
1900    SUBEND
```

```
 10  ! LAG RE-SHAPING SPECTRAL ANALYSIS FOR REAL DATA
 20    T=10000                 !  TOTAL NUMBER OF DATA POINTS
 30    L1=769                  !  NUMBER OF DATA POINTS PER PIECE
 40    L2max=250               !  MAXIMUM LAG WEIGHTING LENGTH
 50    N1=1024                 !  SIZE OF FIRST-STAGE FFT N1>=L1+L2max
 60    DATA .355768,.487396,.144232,.012604   !  LAG WEIGHTING COEFFICIENTS
 70  ! TR 6239, page 16, figure 12: -46.66 dB sidelobes, 9 dB/octave decay
 80    DIM X(0:16383),Y(0:16383),Xa(0:8191)
 90    DOUBLE T,L1,L2max,N1,N1m,K,Ks,Ns,L2,N2,N2m     !  INTEGERS
100    IF N1>=L1+L2max THEN 140
110    PRINT "N1 INCREASED, SO AS TO BE AT LEAST L1+L2max"
120    N1m=INT(LOG(L1+L2max)/LOG(2))+1
130    N1=2^N1m
140    N1m=N1-1
150    REDIM X(0:N1m),Y(0:N1m),Xa(0:N1m)
160    K=INT(T/L1)                     !  NUMBER OF DATA SEGMENTS
170    PRINT "T =";T;"   L1 =";L1;"   L2max =";L2max;"   N1 =";N1;"   K =";K
180    PRINT "USED";K*L1;"OF THE TOTAL NUMBER OF DATA POINTS,";T
190    READ A0,A1,A2,A3
200    A=1./(A0+A1+A2+A3)              !  NORMALIZE LAG WEIGHTS
210    A0=A0*A
220    A1=A1*A
230    A2=A2*A
240    A3=A3*A
250    MAT Xa=(0.)
260    FOR Ks=1 TO K
270    CALL Data(Ks,L1,X(*))           !  L1 DATA POINTS AT A TIME
280    FOR Ns=L1 TO N1m
290    X(Ns)=0.
300    NEXT Ns
310    MAT Y=(0.)
320    CALL Fft14z(N1,X(*),Y(*))       !  INTO FREQUENCY DOMAIN
330    FOR Ns=0 TO N1m
340    Xa(Ns)=Xa(Ns)+X(Ns)*X(Ns)+Y(Ns)*Y(Ns)   !  POWER AVERAGING
350    NEXT Ns
360    NEXT Ks
370    MAT Y=(0.)
380    CALL Fft14z(N1,Xa(*),Y(*))      !  INTO LAG DOMAIN
390    FOR Ns=0 TO L1-1
400    Xa(Ns)=Xa(Ns)*L1/(L1-Ns)        !  DIVIDE BY CORRELATION
410    NEXT Ns                         !  OF TEMPORAL WEIGHTING
420    BEEP
430    INPUT "L2 =",L2         !  LAG WEIGHTING LENGTH L2<L1, L2<=N1-L1
440    INPUT "N2 =",N2         !  SIZE OF SECOND-STAGE FFT N2 (>L2*10 IS GOOD)
450    IF L2<L1 THEN 480
460    PRINT "L2 REDUCED TO L1-1, TO AVOID DIVISION BY ZERO"
470    L2=L1-1
480    IF L2<=L2max THEN 510
490    PRINT "L2 REDUCED TO L2max, TO AVOID WRAP-AROUND REGION"
500    L2=L2max
510    IF N2>L2+L2 THEN 550
520    PRINT "N2 INCREASED, SO AS TO BE GREATER THAN L2*2"
530    N2m=INT(LOG(L2+L2+1)/LOG(2))+1
540    N2=2^N2m
550    PRINT "L2 =";L2;"     N2 =";N2
560    N2m=N2-1
570    REDIM X(0:N2m),Y(0:N2m)
```

```
580     A=PI/L2
590     X(0)=Xa(0)
600     FOR Ns=1 TO L2
610     B=Ns*A
620     W=A0+A1*COS(B)+A2*COS(B+B)+A3*COS(B+B+B)
630     X(Ns)=X(N2-Ns)=Xa(Ns)*W         !  LAG WEIGHTING
640     NEXT Ns
650     FOR Ns=L2+1 TO N2m-L2
660     X(Ns)=0.
670     NEXT Ns
680     MAT Y=(0.)
690     CALL Fft14z(N2,X(*),Y(*))       !  INTO FREQUENCY DOMAIN
700     MAT X=X/(FLT(K)*L1*N1*N2)
710     Big=MAX(X(*))
720     Db=LGT(Big)*10.
730     PRINT "Big =";Big;"     dB max =";Db
740     PLOTTER IS "GRAPHICS"
750     GRAPHICS ON
760     WINDOW 0.,N2/2,-70.,0.
770     GRID N2/8,10.
780     FOR Ns=0 TO N2/2
790     W=MAX(X(Ns),1.E-20)
800     PLOT Ns,LGT(W)*10.-Db
810     NEXT Ns
820     PENUP
830     GOTO 430
840     END
850     !
860     SUB Fft14z(DOUBLE N,REAL X(*),Y(*)) !  N=2^INTEGER<=2^14=16384; 0 SUBS
870   ! This SUB is listed above.
1670    SUBEND
1680    !
1690    SUB Data(DOUBLE Ks,L1,REAL X(*))
1700    DOUBLE J1,J2,J
1710    W1=2.*PI*.25            !  TONE FREQUENCY 1
1720    W2=2.*PI*.265           !  TONE FREQUENCY 2
1730    T1=.31                  !  TONE PHASE 1
1740    T2=.77                  !  TONE PHASE 2
1750    Db2=-30.                !  RELATIVE TONE STRENGTH
1760    A2=10.^(Db2/20.)
1770    J2=Ks*L1-1
1780    J1=J2-L1+1
1790    FOR J=J1 TO J2
1800    P1=W1*J+T1
1810    P2=W2*J+T2
1820    X(J-J1)=COS(P1)+A2*COS(P2)+(RND-.5)*.316
1830  ! RND-.5 has power 1/12
1840    NEXT J
1850    SUBEND
```

REFERENCES

1. A. H. Nuttall, Spectral Analysis via Quadratic Frequency-Smoothing of Fourier-Transformed Overlapped Weighted Data Segments, NUSC Technical Report 6459, 1 June 1981. Also, A. H. Nuttall and G. C. Carter, "Spectral Estimation Using Combined Time and Lag Weighting," Special Issue on Spectral Estimation, Invited Paper in Proceedings IEEE, vol. 70, no. 9, pp. 1115-1125, September 1982.
2. M. S. Bartlett, An Introduction to Stochastic Processes, with Special Reference to Methods and Applications, Cambridge University Press, Cambridge, 1953.
3. R. B. Blackman and J. W. Tukey, The Measurement of Power Spectra from the Point of View of Communications Engineering, Dover Publications, Inc., New York, 1959.
4. E. Parzen, "Mathematical Considerations in the Estimation of Spectra," Technometrics, vol. 3, 1961.
5. R. B. Blackman, Data Smoothing and Prediction, Addison-Wesley Publishing Company, Inc., Reading, Mass., 1965.
6. J. S. Bendat and A. G. Piersol, Measurement and Analysis of Random Data, J. Wiley and Sons, Inc., New York, 1966.
7. G. M. Jenkins and D. G. Watts, Spectral Analysis and Its Applications, Holden-Day Company, San Francisco, 1968.

REFERENCES (Cont'd)

8. P. D. Welch, "The Use of FFT for the Estimation of Power Spectra: A Method Based on Time Averaging over Short Modified Periodograms," IEEE Transactions on Audio and Electroacoustics, vol. AU-15, no. 2, June 1967, pp. 70-73.

9. C. Bingham, M. D. Godfrey, and J. W. Tukey, "Modern Techniques of Power Spectrum Estimation," IEEE Transactions on Audio and Electroacoustics, vol. AU-15, no. 2, June 1967.

10. A. H. Nuttall, Spectral Estimation by Means of Overlapped Fast Fourier Transform Processing of Windowed Data, NUSC Report No. 4169, 13 October 1971.

11. A. H. Nuttall, Estimation of Cross-Spectra via Overlapped Fast Fourier Transform Processing, NUSC Technical Report 4169-S, 11 July 1975.

12. A. H. Nuttall, Minimum-Bias Windows for Spectral Estimation by Means of Overlapped Fast Fourier Transform Processing, NUSC Technical Report 4513, 11 April 1973.

13. A. H. Nuttall, Probability Distribution of Spectral Estimates Obtained via Overlapped FFT Processing of Windowed Data, NUSC Technical Report 5529, 3 December 1976.

14. A. H. Nuttall and G. C. Carter, "A Generalized Framework for Power Spectral Estimation," IEEE Transactions on Acoustics, Speech, and Signal Processing, vol. ASSP-28, no. 3, pp. 334-335, June 1980.

REFERENCES (Cont'd)

15. G. C. Carter and A. H. Nuttall, "A Brief Summary of a Generalized Framework for Spectral Estimation," Signal Processing, vol. 2, no. 4, pp. 387-390, October 1980.

16. G. C. Carter and A. H. Nuttall, "On the Weighted Overlapped Segment-Averaging Method for Power Spectral Estimation," Proceedings IEEE, vol. 68, no. 10, pp. 1352-1354, October 1980.

17. A. H. Nuttall, "Reconstruction of Power Spectral Estimates," NUSC Technical Memorandum 781051, 6 March 1978.

18. A. H. Nuttall, "Some Windows with Very Good Sidelobe Behavior," IEEE Trans. on Acoustics, Speech, and Signal Processing, vol. ASSP-29, no. 1, pp. 84-91, February 1981. Also NUSC Technical Report 6239, 9 April 1980.

19. F. J. Harris, "On the Use of Windows for Harmonic Analysis with the Discrete Fourier Transform," Proc. IEEE, vol. 66, no. 1, pp. 51-83, January 1978.

INITIAL DISTRIBUTION LIST

Addressee	No. of Copies
ASN (RE&S)	1
OUSDR&E (Research & Advanced Technology)	2
Deputy USDR&E (Res & Adv Technology)	1
Deputy USDR&E (Dir Elect & Phys Sc)	1
OASN, Spec Dep for Adv Concept	1
Principal Dep Assist Secretary (Research)	1
OASN, Dep Assist Secretary (Res & Applied Space Tech)	1
ONR, ONR-100, -102, -200, -400, -410, -422, -425AC, -430	8
CNO, OP-098, -941, -951	3
DIA, DT-2C	1
NRL	1
NRL, USRD	1
NORDA	1
USOC, Code 241, 240	2
SUBBASE LANT	1
NAVSUBSUPACNLON	1
OCEANAV	1
NAVOCEANO, Code 02 (1)	2
NAVELECSYSCOM, ELEX 03, 310	2
NAVSEASYSCOM, SEA-00, -05R, 06F, -63R, -92R	5
NAVAIRDEVCEN, Warminster	1
NAVAIRDEVCEN, Key West	1
NOSC, Code 8302, 6565 (Library)	2
NAVWPNSCEN	1
NCSC, Code 724	1
NAVCIVENGRLAB	1
NAVSWC	1
NAVSURFWPNCEN, Code U31	1
NISC	1
CNET, Code 017	1
CNTT	1
NAVSUBSCOL	1
NAVTRAEQUIPCENT, Technical Library	1
NAVPGSCOL	1
NAVWARCOL	1
NETC	1
APL/UW, SEATTLE	1
ARL/PENN STATE, STATE COLLEGE	1
CENTER FOR NAVAL ANALYSES (ACQUISITION UNIT)	1
DTIC	12
DARPA	1
NOAA/ERL	1
NATIONAL RESEARCH COUNCIL	1
WEAPON SYSTEM EVALUATION GROUP	1
WOODS HOLE OCEANOGRAPHIC INSTITUTION	1
ENGINEERING SOCIETIES LIB, UNITED ENGRG CTR	1
NATIONAL INSTITUTE OF HEALTH	1
ARL, UNIV OF TEXAS	1

INITIAL DISTRIBUTION LIST

Addressee	No. of Copies
MARINE PHYSICAL LAB, SCRIPPS	1
UNIVERSITY OF CALIFORNIA, SAN DIEGO	1
NAVSURWEACTR	1
DELSI	1
INTERMS INC.	1
MAR INC.	1
D-K DYN INC.	1
BB&N, CAMBRIDGE, MA	1
EWASCTRI	1
HYDROINC (D. Clark)	1
SUMRESCR (M. Henry)	1
ANALTECH INC. (G. Bourgond)	1
ANALTECHNS	1
GENPHYCORP (M. Bauer)	1
EDOCORP (J. Vincenzo)	1
OPERRES INC. (Dr. V. P. Simmons)	1
TRA CORP. (J. Wilkinson)	1
BB&N INC., SAN DIEGO, CA	1
NETS (R. Medeiros)	1
GESY (D. Bates)	1
OCNR, Code 30	1